BNL-113654-2017-TECH
C-A/AP/583;BNL-113654-2017-IR

Emittance growth due to multiple passes through H-minus stripping foil in Booster

C. J. Gardner

March 2017

Collider Accelerator Department
Brookhaven National Laboratory

U.S. Department of Energy
USDOE Office of Science (SC), Nuclear Physics (NP) (SC-26)

DISCLAIMER

BNL-113654-2017-IR

C-A/AP/583
March 2017

Emittance growth due to multiple passes through the H-minus stripping foil in Booster

C.J. Gardner

Collider-Accelerator Department
Brookhaven National Laboratory
Upton, NY 11973

U.S. Department of Energy
Office of Science, Office of Nuclear Physics

Emittance Growth due to Multiple Passes through the H-minus Stripping Foil in Booster

C.J. Gardner

March 2, 2017

Expressions for transverse emittance growth due to turn-by-turn passes through the H-minus stripping foil in Booster are developed here from simple principles of statistics and simple assumptions about the initial distribution of particles incident on the foil. These are meant to complement work already presented by Zeno [1, 2, 3] and Brown [4]. The expressions show that while the average emittance $\langle E \rangle$ of the distribution simply increases linearly with turn number, the emittance $\mathcal{E}$ based on the mean square particle position does so with an additional oscillatory term that depends on the machine tune. It is shown that this term can be ignored as long as the turn number is sufficiently large and the tune is sufficiently far from integer and half-integer values. Under these conditions the relation between $\langle E \rangle$ and $\mathcal{E}$ is simply $\langle E \rangle = 2\,\mathcal{E}$. This relation is shown to hold for a Gaussian distribution that is matched to the machine lattice.

Two symmetry conditions which help characterize the particle distribution are identified. These provide justification for calling $\mathcal{E}$ an emittance. It is shown that if the conditions are satisfied by the initial distribution, they will not be satisfied after a single traversal of the foil and one turn around the machine. However, on subsequent turns the distribution can (and does) return to satisfying the conditions. Moreover, for sufficiently large turn number, the symmetry conditions are approximately satisfied.

As already noted in [4], the emittance growth per turn is proportional to the lattice beta at the foil and the mean square angular kick received by protons passing through the foil. We take the former to be 5 m. The latter is obtained from simulations performed with the code TRIM [5]. Having these numbers in hand, actual numbers for emittance growth are presented.

The reader may wish to start with Section 11 and refer to previous sections as needed or desired.

1 Notation and Definitions

We use the subscript ni to refer to the ith particle on the nth turn around the machine.

Let X_{ni} and X'_{ni} be the position and angle of the ith particle **just upstream** of the foil on the nth turn around the machine.

Let X^d_{ni} and X'^d_{ni} be the position and angle of the ith particle **just downstream** of the foil on the nth turn around the machine.

Let α, β, γ be the Courant-Snyder parameters of the machine lattice at the foil. These satisfy

$$\beta\gamma - \alpha^2 = 1. \tag{1}$$

The Courant-Snyder invariant of the ith particle **just upstream** of the foil on the nth turn around the machine is then

$$E_{ni} = \gamma X_{ni}^2 + 2\alpha X_{ni} X'_{ni} + \beta X'^2_{ni}. \tag{2}$$

The emittance of the particle is πE_{ni}, but for convenience we simply call E_{ni} the emittance.

Similarly, the Courant-Snyder invariant of the ith particle **just downstream** of the foil on the nth turn around the machine is

$$E^d_{ni} = \gamma \left(X^d_{ni}\right)^2 + 2\alpha X^d_{ni} X'^d_{ni} + \beta \left(X'^d_{ni}\right)^2. \tag{3}$$

Equations (2) and (3) can be transformed into equations for circles by introducing coordinates

$$Y_{ni} = \alpha X_{ni} + \beta X'_{ni} \tag{4}$$

$$Y^d_{ni} = \alpha X^d_{ni} + \beta X'^d_{ni}. \tag{5}$$

With the help of (1), one obtains

$$\beta E_{ni} = X_{ni}^2 + Y_{ni}^2 \tag{6}$$

$$\beta E^d_{ni} = \left(X^d_{ni}\right)^2 + \left(Y^d_{ni}\right)^2. \tag{7}$$

For any particle parameter V_{ni}, we define its average over all the particles on the nth turn around the machine to be

$$\langle V_n \rangle = \frac{1}{M} \sum_{i=1}^{M} V_{ni} \tag{8}$$

where M is the number of particles.

2 Recurrence Relation for Single Particle Emittance

Upon passing through the foil on the nth turn around the machine, the ith particle receives an angular kick ϕ_{ni}. We assume that the particle position is unchanged. Thus

$$X_{ni}^d = X_{ni} \tag{9}$$

and

$$X_{ni}'^d = X_{ni}' + \phi_{ni} \tag{10}$$

which gives

$$Y_{ni}^d = Y_{ni} + \beta\phi_{ni} \tag{11}$$

$$\left(Y_{ni}^d\right)^2 = Y_{ni}^2 + 2\beta Y_{ni}\phi_{ni} + \beta^2\phi_{ni}^2 \tag{12}$$

$$\beta E_{ni}^d = X_{ni}^2 + Y_{ni}^2 + 2\beta Y_{ni}\phi_{ni} + \beta^2\phi_{ni}^2 \tag{13}$$

and

$$E_{ni}^d = E_{ni} + 2Y_{ni}\phi_{ni} + \beta\phi_{ni}^2. \tag{14}$$

On the next turn around the machine we have (just upstream of the foil)

$$X_{mi} = CX_{ni}^d + SY_{ni}^d \tag{15}$$

$$Y_{mi} = -SX_{ni}^d + CY_{ni}^d \tag{16}$$

where

$$m = n + 1, \quad C = \cos 2\pi Q, \quad S = \sin 2\pi Q \tag{17}$$

and Q is the machine tune. Thus we have

$$X_{mi}^2 + Y_{mi}^2 = \left(X_{ni}^d\right)^2 + \left(Y_{ni}^d\right)^2 \tag{18}$$

and therefore

$$E_{mi} = E_{ni}^d \tag{19}$$

where

$$\beta E_{mi} = X_{mi}^2 + Y_{mi}^2 \tag{20}$$

$$\beta E_{ni}^d = \left(X_{ni}^d\right)^2 + \left(Y_{ni}^d\right)^2. \tag{21}$$

Using (14) we then have

$$E_{mi} = E_{ni} + 2Y_{ni}\phi_{ni} + \beta\phi_{ni}^2 \tag{22}$$

where $m = n + 1$. This gives the turn-by-turn evolution of the single particle emittance.

3 Recurrence Relation for Average Emittance

Averaging (22) over all the particles according to (8), we have

$$\langle E_{n+1}\rangle = \langle E_n\rangle + 2\langle Y_n\phi_n\rangle + \beta\left\langle \phi_n^2\right\rangle. \tag{23}$$

Similarly averaging (9), (11), (15), and (16) we have

$$\left\langle X_n^d\right\rangle = \langle X_n\rangle \tag{24}$$

$$\left\langle Y_n^d\right\rangle = \langle Y_n\rangle + \beta\langle\phi_n\rangle \tag{25}$$

and

$$\langle X_{n+1}\rangle = C\langle X_n\rangle + S\langle Y_n\rangle + S\beta\langle\phi_n\rangle \tag{26}$$

$$\langle Y_{n+1}\rangle = -S\langle X_n\rangle + C\langle Y_n\rangle + C\beta\langle\phi_n\rangle. \tag{27}$$

We shall assume that the angular kick ϕ_{ni} averaged over all particles is zero. Thus

$$\langle\phi_n\rangle = 0 \tag{28}$$

for all n. This gives

$$\left\langle Y_n^d\right\rangle = \langle Y_n\rangle \tag{29}$$

and

$$\langle X_{n+1}\rangle = C\langle X_n\rangle + S\langle Y_n\rangle \tag{30}$$

$$\langle Y_{n+1}\rangle = -S\langle X_n\rangle + C\langle Y_n\rangle \tag{31}$$

for all n. It follows that if

$$\langle X_0\rangle = 0, \quad \langle Y_0\rangle = 0 \tag{32}$$

then

$$\langle X_n\rangle = 0, \quad \langle Y_n\rangle = 0 \tag{33}$$

for all $n > 0$. **We shall assume that (32) and (33) are always satisfied.**

We assume further that Y_{ni} and ϕ_{ni} are uncorrelated. It follows that [6]

$$\langle Y_n\phi_n\rangle = 0. \tag{34}$$

Equation (23) then becomes

$$\langle E_{n+1}\rangle = \langle E_n\rangle + \beta\left\langle \phi_n^2\right\rangle. \tag{35}$$

This gives the turn-by-turn evolution of the average emittance.

4 Recurrence Relations for Quadratic Terms

Using (9) and (11) in (15) and (16) we have

$$X_{mi} = (CX_{ni} + SY_{ni}) + S\beta\phi_{ni} \tag{36}$$

$$Y_{mi} = (-SX_{ni} + CY_{ni}) + C\beta\phi_{ni} \tag{37}$$

which gives

$$\begin{aligned} X_{mi}^2 &= C^2X_{ni}^2 + S^2Y_{ni}^2 + 2CSX_{ni}Y_{ni} \\ &+ 2S\beta\left(CX_{ni} + SY_{ni}\right)\phi_{ni} + S^2\beta^2\phi_{ni}^2 \end{aligned} \tag{38}$$

$$\begin{aligned} Y_{mi}^2 &= S^2X_{ni}^2 + C^2Y_{ni}^2 - 2CSX_{ni}Y_{ni} \\ &+ 2C\beta\left(-SX_{ni} + CY_{ni}\right)\phi_{ni} + C^2\beta^2\phi_{ni}^2 \end{aligned} \tag{39}$$

$$\begin{aligned} X_{mi}Y_{mi} &= CS\left(Y_{ni}^2 - X_{ni}^2\right) + \left(C^2 - S^2\right)X_{ni}Y_{ni} + SC\beta^2\phi_{ni}^2 \\ &+ \left\{C\left(CX_{ni} + SY_{ni}\right) + S\left(-SX_{ni} + CY_{ni}\right)\right\}\beta\phi_{ni} \end{aligned} \tag{40}$$

$$\begin{aligned} X_{mi}Y_{mi} &= CS\left(Y_{ni}^2 - X_{ni}^2\right) + \left(C^2 - S^2\right)X_{ni}Y_{ni} + SC\beta^2\phi_{ni}^2 \\ &+ \left\{\left(C^2 - S^2\right)X_{ni} + 2CSY_{ni}\right\}\beta\phi_{ni} \end{aligned} \tag{41}$$

where

$$m = n + 1. \tag{42}$$

As before we assume that

$$\langle\phi_n\rangle = 0, \quad \langle X_n\rangle = 0, \quad \langle Y_n\rangle = 0 \tag{43}$$

for all n. We assume further that both X_{ni} and Y_{ni} are uncorrelated with ϕ_{ni}. This implies [6]

$$\langle X_n\phi_n\rangle = 0, \quad \langle Y_n\phi_n\rangle = 0. \tag{44}$$

Averaging over the particles we then have

$$\left\langle X_{n+1}^2\right\rangle = C^2\left\langle X_n^2\right\rangle + S^2\left\langle Y_n^2\right\rangle + 2CS\left\langle X_nY_n\right\rangle + S^2\beta^2\left\langle\phi_n^2\right\rangle \tag{45}$$

$$\left\langle Y_{n+1}^2\right\rangle = S^2\left\langle X_n^2\right\rangle + C^2\left\langle Y_n^2\right\rangle - 2CS\left\langle X_nY_n\right\rangle + C^2\beta^2\left\langle\phi_n^2\right\rangle \tag{46}$$

and

$$\begin{aligned}\langle X_{n+1}Y_{n+1}\rangle &= CS\left\langle Y_n^2\right\rangle - CS\left\langle X_n^2\right\rangle \\ &+ \left(C^2-S^2\right)\langle X_nY_n\rangle + SC\beta^2\left\langle\phi_n^2\right\rangle. \end{aligned} \tag{47}$$

These equations give the turn-by-turn evolution of the quadratic terms.

Note that adding (45) and (46) gives

$$\left\langle X_{n+1}^2\right\rangle + \left\langle Y_{n+1}^2\right\rangle = \left\langle X_n^2\right\rangle + \left\langle Y_n^2\right\rangle + \beta^2\left\langle\phi_n^2\right\rangle. \tag{48}$$

Using

$$\beta\langle E_{n+1}\rangle = \left\langle X_{n+1}^2\right\rangle + \left\langle Y_{n+1}^2\right\rangle \tag{49}$$

$$\beta\langle E_n\rangle = \left\langle X_n^2\right\rangle + \left\langle Y_n^2\right\rangle \tag{50}$$

we then have

$$\beta\langle E_{n+1}\rangle = \beta\langle E_n\rangle + \beta^2\left\langle\phi_n^2\right\rangle \tag{51}$$

which is the same as (35).

5 Symmetric Particle Distribution

If

$$\left\langle X_n^2\right\rangle = \left\langle Y_n^2\right\rangle \tag{52}$$

and

$$\langle X_nY_n\rangle = 0 \tag{53}$$

then we say that the particle distribution is **symmetric** on the nth turn around the machine.

Using these equations in (45), (46), and (47) we have, on the next turn,

$$\left\langle X_{n+1}^2\right\rangle = \left\langle X_n^2\right\rangle + S^2\beta^2\left\langle\phi_n^2\right\rangle \tag{54}$$

$$\left\langle Y_{n+1}^2\right\rangle = \left\langle Y_n^2\right\rangle + C^2\beta^2\left\langle\phi_n^2\right\rangle \tag{55}$$

and

$$\langle X_{n+1}Y_{n+1}\rangle = SC\beta^2\left\langle\phi_n^2\right\rangle \tag{56}$$

where

$$C = \cos 2\pi Q, \quad S = \sin 2\pi Q. \tag{57}$$

Here we see that if $\langle \phi_n^2 \rangle$ is zero then the distribution remains symmetric. However, if $\langle \phi_n^2 \rangle$ is nonzero then there **is no** value of Q that gives **both**

$$\left\langle X_{n+1}^2 \right\rangle = \left\langle Y_{n+1}^2 \right\rangle \tag{58}$$

and

$$\langle X_{n+1} Y_{n+1} \rangle = 0. \tag{59}$$

The particle distribution is no longer symmetric. In **Section 7** it will be shown that the distribution can return to being symmetric after a certain number of turns.

We obtain the symmetry conditions (52) and (53) **in terms of the original coordinates** by returning to equation (4). We have

$$Y_{ni} = \alpha X_{ni} + \beta X'_{ni} \tag{60}$$

$$X_{ni} Y_{ni} = \alpha X_{ni}^2 + \beta X_{ni} X'_{ni} \tag{61}$$

and

$$Y_{ni}^2 = \alpha^2 X_{ni}^2 + 2\alpha\beta X_{ni} X'_{ni} + \beta^2 X_{ni}'^2. \tag{62}$$

Averaging over the particles then gives

$$\beta \left\langle X_n X'_n \right\rangle = \langle X_n Y_n \rangle - \alpha \left\langle X_n^2 \right\rangle \tag{63}$$

and

$$\beta^2 \left\langle X_n'^2 \right\rangle = \left\langle Y_n^2 \right\rangle - \alpha^2 \left\langle X_n^2 \right\rangle - 2\alpha\beta \left\langle X_n X'_n \right\rangle. \tag{64}$$

Using (63) in (64) gives

$$\beta^2 \left\langle X_n'^2 \right\rangle = \left\langle Y_n^2 \right\rangle - \alpha^2 \left\langle X_n^2 \right\rangle - 2\alpha \left\langle X_n Y_n \right\rangle + 2\alpha^2 \left\langle X_n^2 \right\rangle \tag{65}$$

$$\beta^2 \left\langle X_n'^2 \right\rangle = \left\langle Y_n^2 \right\rangle + \alpha^2 \left\langle X_n^2 \right\rangle - 2\alpha \left\langle X_n Y_n \right\rangle. \tag{66}$$

If the distribution is symmetric on the nth turn around the machine we have

$$\left\langle X_n^2 \right\rangle = \left\langle Y_n^2 \right\rangle, \quad \langle X_n Y_n \rangle = 0. \tag{67}$$

Equation (63) then becomes

$$\langle X_n X'_n \rangle = -\frac{\alpha}{\beta} \left\langle X_n^2 \right\rangle \tag{68}$$

and, with the help of (1), equation (66) becomes

$$\beta \left\langle X_n'^2 \right\rangle = \gamma \left\langle X_n^2 \right\rangle . \tag{69}$$

These are the symmetry conditions in terms of $\langle X_n^2 \rangle$, $\langle X_n'^2 \rangle$, and $\langle X_n X_n' \rangle$.

Defining

$$\mathcal{E}_n = \frac{1}{\beta} \left\langle X_n^2 \right\rangle \tag{70}$$

we have

$$\left\langle X_n^2 \right\rangle = \mathcal{E}_n \beta \tag{71}$$

and equations (68) and (69) become

$$\langle X_n X_n' \rangle = -\mathcal{E}_n \alpha \tag{72}$$

and

$$\left\langle X_n'^2 \right\rangle = \mathcal{E}_n \gamma. \tag{73}$$

A Gaussian distribution that is matched to the machine lattice is an example of a symmetric distribution and in **Appendix I** is shown to have these properties.

6 Quadratic Terms in Complex Form

Returning to (36) and (37) we have

$$X_{mi} = (CX_{ni} + SY_{ni}) + S\beta\phi_{ni} \tag{74}$$

$$Y_{mi} = (-SX_{ni} + CY_{ni}) + C\beta\phi_{ni} \tag{75}$$

where

$$C = \cos 2\pi Q, \quad S = \sin 2\pi Q \tag{76}$$

and

$$m = n + 1. \tag{77}$$

Equations (74) and (75) can be combined and written in complex form as

$$X_{mi} + iY_{mi} = (C - iS)(X_{ni} + iY_{ni}) + (C - iS)\, i\beta\phi_{ni}. \tag{78}$$

This can be written as

$$Z_{mi} = (C - iS)\,(Z_{ni} + i\beta\phi_{ni}) \tag{79}$$

where

$$Z_{mi} = X_{mi} + iY_{mi} \tag{80}$$

$$Z_{ni} = X_{ni} + iY_{ni}. \tag{81}$$

Defining

$$\psi = 2\pi Q \tag{82}$$

we then have

$$Z_{mi} = e^{-i\psi}\,(Z_{ni} + i\beta\phi_{ni}) \tag{83}$$

$$Z^*_{mi} = e^{i\psi}\,(Z^*_{ni} - i\beta\phi_{ni}) \tag{84}$$

and

$$Z_{mi}Z^*_{mi} = (Z_{ni} + i\beta\phi_{ni})\,(Z^*_{ni} - i\beta\phi_{ni}) \tag{85}$$

$$Z_{mi}Z^*_{mi} = Z_{ni}Z^*_{ni} + i\beta\phi_{ni}\,(Z^*_{ni} - Z_{ni}) + \beta^2\phi^2_{ni} \tag{86}$$

where

$$i\beta\phi_{ni}\,(Z^*_{ni} - Z_{ni}) = 2\beta\phi_{ni}Y_{ni}. \tag{87}$$

Thus, using (44) we have

$$\left\langle Z_{n+1}Z^*_{n+1}\right\rangle = \left\langle Z_nZ^*_n\right\rangle + \beta^2\left\langle\phi^2_n\right\rangle. \tag{88}$$

We also have

$$Z^2_{mi} = e^{-2i\psi}\,(Z_{ni} + i\beta\phi_{ni})\,(Z_{ni} + i\beta\phi_{ni}) \tag{89}$$

$$Z^2_{mi} = e^{-2i\psi}\left(Z^2_{ni} + 2i\beta\phi_{ni}Z_{ni} - \beta^2\phi^2_{ni}\right) \tag{90}$$

where

$$\phi_{ni}Z_{ni} = \phi_{ni}X_{ni} + i\phi_{ni}Y_{ni}. \tag{91}$$

Using (44) again we have

$$\left\langle Z^2_{n+1}\right\rangle = \mathcal{Z}\left\langle Z^2_n\right\rangle - \mathcal{Z}\beta^2\left\langle\phi^2_n\right\rangle \tag{92}$$

where

$$\mathcal{Z} = e^{-2i\psi}, \quad \psi = 2\pi Q. \tag{93}$$

Equations (88) and (92) give the turn-by-turn evolution of the quadratic terms in complex form.

7 Summation of Recursive Quadratic Terms

We assume that mean square angular kick $\langle \phi_n^2 \rangle$ is the same on all turns around the machine. Thus we can write

$$\left\langle \phi_n^2 \right\rangle = \left\langle \phi^2 \right\rangle \tag{94}$$

for all n. According to equation (92) we then have

$$\left\langle Z_1^2 \right\rangle = \mathcal{Z} \left\langle Z_0^2 \right\rangle - \mathcal{Z}\beta^2 \left\langle \phi^2 \right\rangle \tag{95}$$

$$\left\langle Z_2^2 \right\rangle = \mathcal{Z}^2 \left\langle Z_0^2 \right\rangle - \left(\mathcal{Z} + \mathcal{Z}^2\right) \beta^2 \left\langle \phi^2 \right\rangle \tag{96}$$

$$\left\langle Z_2^3 \right\rangle = \mathcal{Z}^3 \left\langle Z_0^2 \right\rangle - \left(\mathcal{Z} + \mathcal{Z}^2 + \mathcal{Z}^3\right) \beta^2 \left\langle \phi^2 \right\rangle \tag{97}$$

$$\left\langle Z_2^4 \right\rangle = \mathcal{Z}^4 \left\langle Z_0^2 \right\rangle - \left(\mathcal{Z} + \mathcal{Z}^2 + \mathcal{Z}^3 + \mathcal{Z}^4\right) \beta^2 \left\langle \phi^2 \right\rangle \tag{98}$$

and so on up to

$$\left\langle Z_n^2 \right\rangle = \mathcal{Z}^n \left\langle Z_0^2 \right\rangle - \left(\mathcal{Z} + \mathcal{Z}^2 + \mathcal{Z}^3 + \cdots + \mathcal{Z}^n\right) \beta^2 \left\langle \phi^2 \right\rangle. \tag{99}$$

Here one can use the identity

$$(1 - \mathcal{Z}) \left(\mathcal{Z} + \mathcal{Z}^2 + \mathcal{Z}^3 + \cdots + \mathcal{Z}^n\right) = \mathcal{Z} - \mathcal{Z}^{n+1} \tag{100}$$

which gives, provided $\mathcal{Z} \neq 1$,

$$\left\langle Z_n^2 \right\rangle = \mathcal{Z}^n \left\langle Z_0^2 \right\rangle - \frac{\mathcal{Z}\left(1 - \mathcal{Z}^n\right)}{1 - \mathcal{Z}} \beta^2 \left\langle \phi^2 \right\rangle \tag{101}$$

where

$$\mathcal{Z} = e^{-2i\psi}, \quad \mathcal{Z}^n = e^{-2in\psi}, \quad \psi = 2\pi Q. \tag{102}$$

Similarly, according to (88) we have

$$\langle Z_1 Z_1^* \rangle - \langle Z_0 Z_0^* \rangle = \beta^2 \left\langle \phi^2 \right\rangle \tag{103}$$

$$\langle Z_2 Z_2^* \rangle - \langle Z_1 Z_1^* \rangle = \beta^2 \left\langle \phi^2 \right\rangle \tag{104}$$

$$\langle Z_3 Z_3^* \rangle - \langle Z_2 Z_2^* \rangle = \beta^2 \left\langle \phi^2 \right\rangle \tag{105}$$

$$\langle Z_4 Z_4^* \rangle - \langle Z_3 Z_3^* \rangle = \beta^2 \left\langle \phi^2 \right\rangle \tag{106}$$

and so on up to

$$\langle Z_n Z_n^* \rangle - \langle Z_{n-1} Z_{n-1}^* \rangle = \beta^2 \left\langle \phi^2 \right\rangle. \tag{107}$$

Summing these equations gives

$$\langle Z_n Z_n^* \rangle = \langle Z_0 Z_0^* \rangle + n\beta^2 \left\langle \phi^2 \right\rangle. \tag{108}$$

Returning to real and imaginary components we have

$$Z_{ni} = X_{ni} + iY_{ni} \tag{109}$$

$$Z_{ni}^2 = X_{ni}^2 - Y_{ni}^2 + 2iX_{ni}Y_{ni} \tag{110}$$

$$Z_{ni} Z_{ni}^* = X_{ni}^2 + Y_{ni}^2 \tag{111}$$

and therefore

$$\left\langle Z_n^2 \right\rangle = \left\langle X_n^2 - Y_n^2 + 2iX_n Y_n \right\rangle \tag{112}$$

$$\left\langle Z_0^2 \right\rangle = \left\langle X_0^2 - Y_0^2 + 2iX_0 Y_0 \right\rangle \tag{113}$$

$$\langle Z_n Z_n^* \rangle = \left\langle X_n^2 + Y_n^2 \right\rangle \tag{114}$$

$$\langle Z_0 Z_0^* \rangle = \left\langle X_0^2 + Y_0^2 \right\rangle. \tag{115}$$

Thus we have

$$\left\langle X_n^2 - Y_n^2 + 2iX_n Y_n \right\rangle = \mathcal{Z}^n \left\langle X_0^2 - Y_0^2 + 2iX_0 Y_0 \right\rangle - \mathcal{F}_n \beta^2 \left\langle \phi^2 \right\rangle \tag{116}$$

$$\left\langle X_n^2 + Y_n^2 \right\rangle = \left\langle X_0^2 + Y_0^2 \right\rangle + n\beta^2 \left\langle \phi^2 \right\rangle \tag{117}$$

$$\beta \langle E_n \rangle = \left\langle X_n^2 \right\rangle + \left\langle Y_n^2 \right\rangle \tag{118}$$

$$\beta \langle E_0 \rangle = \left\langle X_0^2 \right\rangle + \left\langle Y_0^2 \right\rangle \tag{119}$$

and

$$\langle E_n \rangle = \langle E_0 \rangle + n\beta \left\langle \phi^2 \right\rangle \tag{120}$$

where

$$\mathcal{F}_n = \frac{\mathcal{Z}\left(1 - \mathcal{Z}^n\right)}{1 - \mathcal{Z}} \tag{121}$$

and

$$\mathcal{Z} = e^{-2i\psi}, \quad \mathcal{Z}^n = e^{-2in\psi}, \quad \psi = 2\pi Q. \tag{122}$$

These equations give the values of

$$\left\langle X_n^2 \right\rangle,\ \left\langle Y_n^2 \right\rangle,\ \langle E_n \rangle,\ \langle X_n Y_n \rangle \tag{123}$$

directly (i.e. without recursive steps) in terms of

$$\left\langle X_0^2 \right\rangle,\ \left\langle Y_0^2 \right\rangle,\ \langle E_0 \rangle,\ \langle X_0 Y_0 \rangle,\ \left\langle \phi^2 \right\rangle,\ \beta^2,\ \mathcal{Z}. \tag{124}$$

Note that for the **special case** in which

$$\mathcal{Z}^n = 1, \quad \mathcal{Z} \neq 1 \tag{125}$$

we have

$$\mathcal{F}_n = 0 \tag{126}$$

and (116) becomes

$$\left\langle X_n^2 \right\rangle - \left\langle Y_n^2 \right\rangle + 2i \langle X_n Y_n \rangle = \left\langle X_0^2 \right\rangle - \left\langle Y_0^2 \right\rangle + 2i \langle X_0 Y_0 \rangle \tag{127}$$

which gives

$$\left\langle X_n^2 \right\rangle - \left\langle Y_n^2 \right\rangle = \left\langle X_0^2 \right\rangle - \left\langle Y_0^2 \right\rangle \tag{128}$$

and

$$\langle X_n Y_n \rangle = \langle X_0 Y_0 \rangle . \tag{129}$$

Thus, if the initial particle distribution is symmetric we have

$$\left\langle X_0^2 \right\rangle = \left\langle Y_0^2 \right\rangle, \quad \langle X_0 Y_0 \rangle = 0 \tag{130}$$

and equations (128) and (129) give

$$\left\langle X_n^2 \right\rangle = \left\langle Y_n^2 \right\rangle, \quad \langle X_n Y_n \rangle = 0. \tag{131}$$

The particle distribution therefore **returns (on the nth turn) to being a symmetric distribution** satisfying (52) and (53). The average emittance, however, continues to increase linearly with turn number according to (120).

8 Emittance from Mean Square Position

Writing (121) as

$$\mathcal{F}_n = \mathcal{A}_n + i\mathcal{B}_n = \frac{\mathcal{Z}\left(1-\mathcal{Z}^n\right)}{1-\mathcal{Z}} \tag{132}$$

where $\mathcal{A}_n$ and $\mathcal{B}_n$ are real, and writing

$$\mathcal{Z}^n = \mathcal{C}_n - i\mathcal{S}_n \tag{133}$$

$$\mathcal{C}_n = \cos 2n\psi, \quad \mathcal{S}_n = \sin 2n\psi, \quad \psi = 2\pi Q \tag{134}$$

we have

$$\mathcal{A}_n + i\mathcal{B}_n = \frac{\mathcal{Z}\left(1-\mathcal{Z}^*\right)\left(1-\mathcal{Z}^n\right)}{\left(1-\mathcal{Z}\right)\left(1-\mathcal{Z}^*\right)} \tag{135}$$

and

$$\mathcal{A}_n + i\mathcal{B}_n = \frac{-\left(1-\mathcal{Z}\right)\left(1-\mathcal{Z}^n\right)}{2\left(1-\mathcal{C}_1\right)} \tag{136}$$

which gives

$$\mathcal{A}_n = \frac{\mathcal{S}_1\mathcal{S}_n}{2\left(1-\mathcal{C}_1\right)} - \frac{1}{2}\left(1-\mathcal{C}_n\right) \tag{137}$$

$$\mathcal{B}_n = -\frac{\mathcal{S}_n}{2} - \frac{\mathcal{S}_1\left(1-\mathcal{C}_n\right)}{2\left(1-\mathcal{C}_1\right)}. \tag{138}$$

These coefficients, the real and imaginary components of $\mathcal{F}_n$, **simply oscillate** as n increases; they do not grow without bound.

The real and imaginary components of (116) are then

$$\left\langle X_n^2 - Y_n^2 \right\rangle = \mathcal{C}_n \left\langle X_0^2 - Y_0^2 \right\rangle + 2\mathcal{S}_n \left\langle X_0 Y_0 \right\rangle - \mathcal{A}_n \beta^2 \left\langle \phi^2 \right\rangle \tag{139}$$

$$2\left\langle X_n Y_n \right\rangle = 2\mathcal{C}_n \left\langle X_0 Y_0 \right\rangle - \mathcal{S}_n \left\langle X_0^2 - Y_0^2 \right\rangle - \mathcal{B}_n \beta^2 \left\langle \phi^2 \right\rangle. \tag{140}$$

Adding (139) and (117) gives

$$\begin{aligned} 2\left\langle X_n^2 \right\rangle &= \mathcal{C}_n \left\langle X_0^2 - Y_0^2 \right\rangle + \left\langle X_0^2 + Y_0^2 \right\rangle \\ &+ 2\mathcal{S}_n \left\langle X_0 Y_0 \right\rangle + \left(n - \mathcal{A}_n\right)\beta^2 \left\langle \phi^2 \right\rangle. \end{aligned} \tag{141}$$

Similarly, subtracting (139) from (117) gives

$$\begin{aligned} 2\left\langle Y_n^2 \right\rangle &= \left\langle X_0^2 + Y_0^2 \right\rangle - \mathcal{C}_n \left\langle X_0^2 - Y_0^2 \right\rangle + \\ &- 2\mathcal{S}_n \left\langle X_0 Y_0 \right\rangle + \left(n + \mathcal{A}_n\right)\beta^2 \left\langle \phi^2 \right\rangle. \end{aligned} \tag{142}$$

Assuming that the particle distribution is **initially symmetric**, we have

$$\left\langle X_0^2 \right\rangle = \left\langle Y_0^2 \right\rangle, \quad \langle X_0 Y_0 \rangle = 0 \tag{143}$$

and equations (141), (142), and (140) become

$$\left\langle X_n^2 \right\rangle = \left\langle X_0^2 \right\rangle + \frac{1}{2}\left(n - \mathcal{A}_n\right)\beta^2 \left\langle \phi^2 \right\rangle \tag{144}$$

$$\left\langle Y_n^2 \right\rangle = \left\langle Y_0^2 \right\rangle + \frac{1}{2}\left(n + \mathcal{A}_n\right)\beta^2 \left\langle \phi^2 \right\rangle \tag{145}$$

$$2\left\langle X_n Y_n \right\rangle = -\mathcal{B}_n \beta^2 \left\langle \phi^2 \right\rangle. \tag{146}$$

Here we see that

$$\left\langle X_n^2 \right\rangle = \left\langle Y_n^2 \right\rangle, \quad \langle X_n Y_n \rangle = 0 \tag{147}$$

if and only if

$$\mathcal{A}_n = 0, \quad \mathcal{B}_n = 0. \tag{148}$$

Moreover, since the coefficient $\mathcal{A}_n$ simply oscillates, the terms proportional to $\mathcal{A}_n$ in (144) and (145) can be ignored if n is sufficiently large. We then have the approximation

$$\left\langle X_n^2 \right\rangle \approx \left\langle Y_n^2 \right\rangle. \tag{149}$$

Compared to $\langle X_n^2 \rangle$ and $\langle Y_n^2 \rangle$, the skew term $\langle X_n Y_n \rangle$ also can be ignored for sufficiently large n. We then can write

$$\langle X_n Y_n \rangle \approx 0 \tag{150}$$

and we see that (for sufficiently large n) the distribution is essentially symmetric. Using

$$\beta \langle E_n \rangle = \left\langle X_n^2 \right\rangle + \left\langle Y_n^2 \right\rangle \tag{151}$$

and the definition

$$\mathcal{E}_n = \frac{1}{\beta}\left\langle X_n^2 \right\rangle \tag{152}$$

we then have the approximation

$$\langle E_n \rangle \approx 2\mathcal{E}_n. \tag{153}$$

This shows that $\mathcal{E}_n$ **can be taken as a measure of the distribution emittance**. This is useful because an actual number for $\mathcal{E}_n$ can be obtained by measuring the mean square position $\langle X_n^2 \rangle$.

9 Relation between $\mathcal{E}_n$ and Average Emittance

Using (152) in (144), we have

$$\mathcal{E}_n = \mathcal{E}_0 + \frac{1}{2}(n - \mathcal{A}_n)\,\beta\left\langle \phi^2 \right\rangle \tag{154}$$

which is to be compared with the average emittance

$$\langle E_n \rangle = \langle E_0 \rangle + n\beta\left\langle \phi^2 \right\rangle \tag{155}$$

where

$$\beta\,\langle E_n \rangle = \left\langle X_n^2 \right\rangle + \left\langle Y_n^2 \right\rangle \tag{156}$$

$$\beta\,\langle E_0 \rangle = \left\langle X_0^2 \right\rangle + \left\langle Y_0^2 \right\rangle. \tag{157}$$

Using the first of equations (143), we have

$$\langle E_0 \rangle = \frac{2}{\beta}\left\langle X_0^2 \right\rangle \tag{158}$$

and therefore

$$\langle E_0 \rangle = 2\,\mathcal{E}_0. \tag{159}$$

In **Appendix I** this relation is shown to hold for a Gaussian distribution that is matched to the lattice.

Using (159) together with (154) and (155) gives

$$2\,\mathcal{E}_n = \langle E_n \rangle - \mathcal{A}_n\,\beta\left\langle \phi^2 \right\rangle \tag{160}$$

which shows that $2\,\mathcal{E}_n$ evolves as the average emittance plus an oscillatory term. We can also write

$$\langle E_n \rangle = 2\,\mathcal{E}_n + \mathcal{A}_n\,\beta\left\langle \phi^2 \right\rangle \tag{161}$$

which shows that the average emittance can be obtained from measurements via equation (152). These equations show that

$$\langle E_n \rangle = 2\,\mathcal{E}_n \tag{162}$$

if and only if

$$\mathcal{A}_n = 0. \tag{163}$$

Here again one can argue that for sufficiently large n, the terms proportional to $\mathcal{A}_n$ can be ignored in (160) and (161). This gives the approximation

$$\langle E_n \rangle \approx 2\,\mathcal{E}_n. \tag{164}$$

10 Evolution of Difference and Skew Terms

Here we give a more rigorous demonstration of (149) and (150). Returning to (139) and (140) we have difference and skew terms

$$\left\langle X_n^2 - Y_n^2 \right\rangle = \mathcal{C}_n \left\langle X_0^2 - Y_0^2 \right\rangle + 2\mathcal{S}_n \left\langle X_0 Y_0 \right\rangle - \mathcal{A}_n \beta^2 \left\langle \phi^2 \right\rangle \tag{165}$$

$$2 \left\langle X_n Y_n \right\rangle = 2\mathcal{C}_n \left\langle X_0 Y_0 \right\rangle - \mathcal{S}_n \left\langle X_0^2 - Y_0^2 \right\rangle - \mathcal{B}_n \beta^2 \left\langle \phi^2 \right\rangle. \tag{166}$$

These terms simply oscillate as the average emittance $\langle E_n \rangle$ grows according to (155).

Assuming as before that the particle distribution is initially symmetric, we have

$$\left\langle X_0^2 \right\rangle = \left\langle Y_0^2 \right\rangle, \quad \left\langle X_0 Y_0 \right\rangle = 0 \tag{167}$$

and equations (165) and (166) become

$$\left\langle X_n^2 - Y_n^2 \right\rangle = -\mathcal{A}_n \beta^2 \left\langle \phi^2 \right\rangle \tag{168}$$

$$2 \left\langle X_n Y_n \right\rangle = -\mathcal{B}_n \beta^2 \left\langle \phi^2 \right\rangle \tag{169}$$

where

$$\mathcal{A}_n = \frac{\mathcal{S}_1 \mathcal{S}_n}{2\left(1 - \mathcal{C}_1\right)} - \frac{1}{2}\left(1 - \mathcal{C}_n\right) \tag{170}$$

$$\mathcal{B}_n = -\frac{\mathcal{S}_n}{2} - \frac{\mathcal{S}_1\left(1 - \mathcal{C}_n\right)}{2\left(1 - \mathcal{C}_1\right)} \tag{171}$$

and

$$\mathcal{C}_n = \cos 2n\psi, \quad \mathcal{S}_n = \sin 2n\psi, \quad \psi = 2\pi Q. \tag{172}$$

Whenever

$$\mathcal{Z}^n = 1, \quad \mathcal{Z} \neq 1 \tag{173}$$

we have

$$\mathcal{A}_n = 0, \quad \mathcal{B}_n = 0 \tag{174}$$

and equations (168) and (169) give

$$\left\langle X_n^2 \right\rangle = \left\langle Y_n^2 \right\rangle, \quad \left\langle X_n Y_n \right\rangle = 0. \tag{175}$$

The particle distribution returns to being a symmetric distribution as already noted in **Section 7**. The conditions (173) are satisfied whenever

$$\cos 2n\psi = 1, \quad \cos 2\psi \neq 1 \tag{176}$$

which require

$$2n\psi = 2\pi k, \quad 2\psi \neq 2\pi m \tag{177}$$

where k and m are integers and

$$\psi = 2\pi Q. \tag{178}$$

Dividing (168) and (169) by

$$\left\langle X_n^2 \right\rangle + \left\langle Y_n^2 \right\rangle = \beta \left\langle E_n \right\rangle \tag{179}$$

we have

$$\frac{\left\langle X_n^2 - Y_n^2 \right\rangle}{\left\langle X_n^2 + Y_n^2 \right\rangle} = -\frac{\mathcal{A}_n}{\left\langle E_n \right\rangle} \beta \left\langle \phi^2 \right\rangle \tag{180}$$

and

$$\frac{2 \left\langle X_n Y_n \right\rangle}{\left\langle X_n^2 + Y_n^2 \right\rangle} = -\frac{\mathcal{B}_n}{\left\langle E_n \right\rangle} \beta \left\langle \phi^2 \right\rangle. \tag{181}$$

As the average emittance $\langle E_n \rangle$ grows sufficiently large we therefore have the approximations

$$\frac{\left\langle X_n^2 - Y_n^2 \right\rangle}{\left\langle X_n^2 + Y_n^2 \right\rangle} \approx 0, \quad \frac{2 \left\langle X_n Y_n \right\rangle}{\left\langle X_n^2 + Y_n^2 \right\rangle} \approx 0. \tag{182}$$

This shows again that for sufficiently large turn numbers, the distribution is essentially symmetric.

11 Dependence of Emittance Growth on Tune

According to equation (154) the emittance growth after n passes of injected beam through the H-minus stripping foil is

$$\mathcal{E}_n - \mathcal{E}_0 = \frac{1}{2} \left(n - \mathcal{A}_n \right) \beta \left\langle \phi^2 \right\rangle \tag{183}$$

which we write as

$$\mathcal{E}_n - \mathcal{E}_0 = F(n) \, \beta \left\langle \phi^2 \right\rangle \tag{184}$$

where

$$F(n) = \frac{1}{2} \left(n - \mathcal{A}_n \right) \tag{185}$$

$$\mathcal{A}_n = \frac{\mathcal{S}_1 \mathcal{S}_n}{2 \left(1 - \mathcal{C}_1 \right)} - \frac{1}{2} \left(1 - \mathcal{C}_n \right) \tag{186}$$

and

$$\mathcal{C}_n = \cos 2n\psi, \quad \mathcal{S}_n = \sin 2n\psi, \quad \psi = 2\pi Q. \tag{187}$$

Figures 1 through **12** show plots of $\mathcal{A}_n$, $\mathcal{B}_n$, and $F(n)$ for various values of the tune Q. The main conclusion to be drawn from the Figures is that the oscillatory coefficient $\mathcal{A}_n$ can be ignored in (185) as long as n is sufficiently large and the tune sufficiently far from integer and half-integer values. One then can write

$$F(n) = \frac{1}{2}\, n \tag{188}$$

and the emittance growth (184) becomes simply

$$\mathcal{E}_n - \mathcal{E}_0 = \frac{1}{2}\, n\beta \left\langle \phi^2 \right\rangle . \tag{189}$$

Using

$$\langle E_n \rangle = \langle E_0 \rangle + n\beta \left\langle \phi^2 \right\rangle \tag{190}$$

we then have

$$\langle E_n \rangle - \langle E_0 \rangle = 2\,(\mathcal{E}_n - \mathcal{E}_0)\,. \tag{191}$$

Since the initial distribution is assumed to be symmetric we have

$$\langle E_0 \rangle = 2\,\mathcal{E}_0 \tag{192}$$

which then gives

$$\langle E_n \rangle = 2\,\mathcal{E}_n. \tag{193}$$

12 Lattice beta at the Foil

To obtain an actual number for the emittance growth we need a number for the lattice beta at the H-minus stripping foil. Modeling [4] of the lattice with various excitations of quadrupole trim windings [7] has shown that beta can be made as small as

$$\beta_H = 4.7 \text{ m}, \quad \beta_V = 2.6 \text{ m} \tag{194}$$

in the horizontal and vertical planes, respectively. We will use

$$\beta = 5.0 \text{ m} \tag{195}$$

to evaluate (189). The emittance growth for other values of β can be obtained by simple scaling of (189).

13 Mean Square Angular Kick at the Foil

We also need a number for the mean square angular kick $\langle \phi^2 \rangle$ received by protons passing through the H-minus stripping foil. This depends on the foil material and thickness, as well as the proton kinetic energy. We consider carbon foils of 200, 150, 100, and 50 micrograms per cm^2 thickness. The proton kinetic energy is 200 MeV.

Assuming a Gaussian probability density of angular kicks

$$\rho(\phi) = \left(\frac{1}{2\pi\sigma^2}\right)^{1/2} \exp\left(-\frac{\phi^2}{2\sigma^2}\right) \tag{196}$$

gives

$$\left\langle \phi^2 \right\rangle = \int_{-\infty}^{+\infty} \phi^2 \rho(\phi)\, d\phi = \sigma^2. \tag{197}$$

The root mean square (rms) angular kick for the distribution is then

$$\phi_{\rm rms} = \left\langle \phi^2 \right\rangle^{1/2} = \sigma. \tag{198}$$

For a discrete set of particles one has

$$\phi_{\rm rms} = \left\langle \phi^2 \right\rangle^{1/2} = \left\{ \frac{1}{M} \sum_{i=1}^{M} \phi_i^2 \right\}^{1/2} \tag{199}$$

where M is the number of particles and ϕ_i is the angular kick received by the ith particle.

Angular scattering simulations performed with the code TRIM [5] show that the Gaussian distribution is a reasonable approximation. **Figures 13**, **14**, **15**, and **16** show the results obtained for 200 MeV protons incident on 200, 150, 100, and 50 microgram per cm^2 carbon foils, respectively. The angles $\phi_{\rm rms}$ obtained for these foils are respectively,

$$\underline{0.0344} \text{ and } \underline{0.0331} \text{ mrad} \tag{200}$$

$$\underline{0.0297} \text{ and } \underline{0.0283} \text{ mrad} \tag{201}$$

$$\underline{0.0243} \text{ and } \underline{0.0226} \text{ mrad} \tag{202}$$

$$\underline{0.0165} \text{ and } \underline{0.0154} \text{ mrad.} \tag{203}$$

Here the numbers on the **left** were obtained directly from (199) using the angles ϕ_i generated by the TRIM code. Those on the **right** were obtained

by binning the TRIM data and then fitting the Gaussian (196) to the binned data. In order to get agreement between the left and right numbers, the angular data from TRIM had to be restricted to the range indicated by the fitted Gaussians in the Figures. The details of setting up the TRIM code to generate the angles ϕ_i are given in **Appendix II**.

14 Emittance Growth Numbers

Using (199) we write (189) as

$$\mathcal{E}_n - \mathcal{E}_0 = \frac{1}{2}\, n\beta\, (\phi_{\rm rms})^2 \tag{204}$$

where $\phi_{\rm rms}$ is given by (200), (201), (202), and (203). We use the **left** number given in each of these equations.

Taking

$$n = \underline{100 \text{ turns}} \tag{205}$$

and

$$\beta = \underline{5 \text{ m}} \tag{206}$$

then gives emittance growths

$$\mathcal{E}_n - \mathcal{E}_0 = \underline{0.296,\ \ 0.221,\ \ 0.148,\ \ 0.068}\ \text{mm mrad} \tag{207}$$

for the 200, 150, 100, and 50 microgram per cm^2 foils, respectively.

These numbers are plotted in **Figure 17** and show that the **emittance growth increases linearly with foil thickness**. The slope of the red line in the Figure is

$$\mathcal{M} = 0.296/200 \tag{208}$$

mm mrad per (microgram per cm^2), which gives emittance growth

$$\mathcal{E}_n - \mathcal{E}_0 = \mathcal{M}\mathcal{T} \tag{209}$$

for foil thickness $\mathcal{T}$. The numbers in (207) can be scaled for different values of n and β. For arbitrary n and β we then have

$$\mathcal{E}_n - \mathcal{E}_0 = \left(\frac{n}{100}\right)\left(\frac{\beta}{5}\right)\mathcal{M}\mathcal{T}. \tag{210}$$

If the particle distributions happen to be **Gaussian** (or nearly so) then, as shown in **Appendix I**, the emittances that contain fraction $F = 0.9502$ of the particles are $6\mathcal{E}_0$ and $6\mathcal{E}_n$. The emittance growth (210) then becomes

$$6\mathcal{E}_n - 6\mathcal{E}_0 = \left(\frac{6n}{100}\right)\left(\frac{\beta}{5}\right)\mathcal{MT}. \tag{211}$$

All of the emittances given above are un-normalized. Normalized emittances are obtained by multiplying the un-normalized ones by the relativistic factor $\beta\gamma = 0.68684$ for 200 MeV protons. Equation (211) then becomes

$$(6\mathcal{E}_n - 6\mathcal{E}_0)_N = (0.68684)\left(\frac{6n}{100}\right)\left(\frac{\beta}{5}\right)\mathcal{MT} \tag{212}$$

where the subscript N denotes normalized emittance.

Figure 18 shows $(6\mathcal{E}_n - 6\mathcal{E}_0)_N$ versus turn for a 100 microgram per cm^2 carbon foil. The black, magenta, and blue lines give, respectively, the growth for 5, 8, and 11 m lattice beta at the foil. The revolution period of 200 MeV protons in Booster is 1.1888 microseconds, which gives a time interval of 396 microseconds for the 333 plotted turns.

Figure 19 shows $(6\mathcal{E}_n - 6\mathcal{E}_0)_N$ versus turn for a 200 microgram per cm^2 carbon foil. The black, magenta, and blue lines again give the growth for 5, 8, and 11 m lattice beta at the foil.

The data plotted in these Figures agree at least qualitatively with the data plotted in Figure 8 of Ref. [4]. Measurements of the lattice beta at the H-minus stripping foil, and turn-by-turn measurements of the circulating beam profile at injection would allow for a more precise comparison.

15 Acknowledgment

I would like to thank Peter Thieberger for introducing me to the TRIM code and showing me how to use it.

16 Appendix I

The particle density for a Gaussian distribution that is matched to the machine lattice is

$$\rho(x,x') = \frac{1}{2\pi\epsilon} e^{-E/(2\epsilon)} \tag{213}$$

where

$$E = \gamma x^2 + 2\alpha x x' + \beta x'^2. \tag{214}$$

Using

$$\beta\gamma = 1 + \alpha^2 \tag{215}$$

we have

$$\beta E = x^2 + (\alpha x + \beta x')^2. \tag{216}$$

Define

$$F(w) = \iint \rho(x,x')\, dx dx' \tag{217}$$

where the integral is taken over the region $E \le w^2$.

To evaluate the integral we first transform to Courant-Snyder coordinates

$$\begin{pmatrix} u \\ v \end{pmatrix} = \begin{pmatrix} 1/\sqrt{\beta} & 0 \\ \alpha/\sqrt{\beta} & \sqrt{\beta} \end{pmatrix} \begin{pmatrix} x \\ x' \end{pmatrix}. \tag{218}$$

Then we have

$$u^2 + v^2 = E \tag{219}$$

$$\begin{pmatrix} x \\ x' \end{pmatrix} = \begin{pmatrix} \sqrt{\beta} & 0 \\ -\alpha/\sqrt{\beta} & 1/\sqrt{\beta} \end{pmatrix} \begin{pmatrix} u \\ v \end{pmatrix} \tag{220}$$

$$\frac{\partial x}{\partial u} = \sqrt{\beta}, \quad \frac{\partial x}{\partial v} = 0 \tag{221}$$

$$\frac{\partial x'}{\partial u} = -\frac{\alpha}{\sqrt{\beta}}, \quad \frac{\partial x'}{\partial v} = \frac{1}{\sqrt{\beta}} \tag{222}$$

and

$$\frac{\partial x}{\partial u}\frac{\partial x'}{\partial v} - \frac{\partial x}{\partial v}\frac{\partial x'}{\partial u} = 1 \tag{223}$$

which give

$$F(w) = \frac{1}{2\pi\epsilon} \iint e^{-(u^2+v^2)/(2\epsilon)}\, du dv \tag{224}$$

where the integral is taken over the region $u^2 + v^2 \le w^2$.

Now let

$$u = r\cos\phi, \quad v = r\sin\phi. \tag{225}$$

Then

$$u^2 + v^2 = r^2 \tag{226}$$

$$\frac{\partial u}{\partial r} = \cos\phi, \quad \frac{\partial u}{\partial \phi} = -r\sin\phi \tag{227}$$

$$\frac{\partial v}{\partial r} = \sin\phi, \quad \frac{\partial v}{\partial \phi} = r\cos\phi \tag{228}$$

$$\frac{\partial u}{\partial r}\frac{\partial v}{\partial \phi} - \frac{\partial u}{\partial \phi}\frac{\partial v}{\partial r} = r \tag{229}$$

and

$$F(w) = \frac{1}{2\pi\epsilon}\int_0^w \int_0^{2\pi} e^{-r^2/(2\epsilon)}\, r dr d\phi. \tag{230}$$

Thus

$$F(w) = \frac{1}{\epsilon}\int_0^w e^{-r^2/(2\epsilon)}\, r dr = 1 - e^{-w^2/(2\epsilon)}. \tag{231}$$

This is the fraction of particles with $E \le w^2$. The fraction of particles with

$$\gamma x^2 + 2\alpha x x' + \beta x'^2 \le 6\epsilon \tag{232}$$

is then

$$F = 1 - e^{-3} = 0.9502. \tag{233}$$

Following the same steps, the average of E over the distribution is

$$\langle E\rangle = \iint E\, \rho(x, x')\, dx dx' \tag{234}$$

$$\langle E\rangle = \frac{1}{2\pi\epsilon}\iint \left(u^2 + v^2\right) e^{-(u^2+v^2)/(2\epsilon)}\, du dv \tag{235}$$

$$\langle E\rangle = \frac{1}{2\pi\epsilon}\int_0^\infty \int_0^{2\pi} r^2\, e^{-r^2/(2\epsilon)}\, r dr d\phi \tag{236}$$

and

$$\langle E\rangle = \frac{1}{\epsilon}\int_0^\infty r^3\, e^{-r^2/(2\epsilon)}\, dr. \tag{237}$$

Similarly we have

$$\left\langle E^2 \right\rangle = \iint E^2 \, \rho(x, x') \, dx dx' \tag{238}$$

$$\left\langle E^2 \right\rangle = \frac{1}{2\pi\epsilon} \iint \left(u^2 + v^2 \right)^2 e^{-(u^2+v^2)/(2\epsilon)} \, du dv \tag{239}$$

$$\left\langle E^2 \right\rangle = \frac{1}{2\pi\epsilon} \int_0^\infty \int_0^{2\pi} r^4 \, e^{-r^2/(2\epsilon)} \, r dr d\phi \tag{240}$$

and

$$\left\langle E^2 \right\rangle = \frac{1}{\epsilon} \int_0^\infty r^5 \, e^{-r^2/(2\epsilon)} \, dr. \tag{241}$$

Using the definite integrals [8]

$$\int_0^\infty r^3 e^{-a^2 r^2} \, dr = \frac{1}{2a^4}, \quad \int_0^\infty r^5 e^{-a^2 r^2} \, dr = \frac{1}{a^6} \tag{242}$$

with

$$a^2 = \frac{1}{2\epsilon} \tag{243}$$

we then have

$$\left\langle E^2 \right\rangle = 8\epsilon^2 \tag{244}$$

and

$$\langle E \rangle = 2\epsilon. \tag{245}$$

Thus

$$\left\langle (E - \langle E \rangle)^2 \right\rangle = \left\langle E^2 \right\rangle - \langle E \rangle^2 = 4\epsilon^2 \tag{246}$$

which gives

$$\left\langle (E - \langle E \rangle)^2 \right\rangle = \langle E \rangle^2 \tag{247}$$

and

$$E_{\text{rms}} = \left\{ \left\langle (E - \langle E \rangle)^2 \right\rangle \right\}^{1/2} = \langle E \rangle \, . \tag{248}$$

Since

$$\langle E \rangle = \left\langle \gamma x^2 + 2\alpha x x' + \beta x'^2 \right\rangle \tag{249}$$

we have

$$\langle E \rangle = \gamma \left\langle x^2 \right\rangle + 2\alpha \left\langle x x' \right\rangle + \beta \left\langle x'^2 \right\rangle \tag{250}$$

and therefore

$$\gamma \left\langle x^2 \right\rangle + 2\alpha \left\langle x x' \right\rangle + \beta \left\langle x'^2 \right\rangle = 2\epsilon. \tag{251}$$

Consider now the projections of the distribution $\rho(x, x')$ on the x and x' axes. These are [9]

$$P(x) = \int_{-\infty}^{+\infty} \rho(x, x')\, dx' = \left(\frac{1}{2\pi\epsilon\beta}\right)^{1/2} \exp\left(-\frac{x^2}{2\epsilon\beta}\right) \tag{252}$$

and

$$Q(x') = \int_{-\infty}^{+\infty} \rho(x, x')\, dx = \left(\frac{1}{2\pi\epsilon\gamma}\right)^{1/2} \exp\left(-\frac{x'^2}{2\epsilon\gamma}\right). \tag{253}$$

Using the definite integral [8]

$$\int_{-\infty}^{+\infty} x^2 e^{-a^2x^2} dx = \frac{\sqrt{\pi}}{2a^3} \tag{254}$$

we then have

$$\left\langle x^2 \right\rangle = \int_{-\infty}^{+\infty} x^2 P(x)\, dx = \epsilon\beta \tag{255}$$

and

$$\left\langle x'^2 \right\rangle = \int_{-\infty}^{+\infty} x'^2 Q(x')\, dx' = \epsilon\gamma. \tag{256}$$

Using these results in (251) we have

$$\gamma\,(\epsilon\beta) + 2\alpha\,\langle xx' \rangle + \beta\,(\epsilon\gamma) = 2\epsilon \tag{257}$$

which gives, with the help of (215),

$$\langle xx' \rangle = -\epsilon\alpha. \tag{258}$$

Equations (255), (256), and (258) are in agreement with (71), (73), and (72), respectively.

Finally, defining

$$y = \alpha x + \beta x' \tag{259}$$

we have

$$\langle xy \rangle = \alpha \left\langle x^2 \right\rangle + \beta \langle xx' \rangle \tag{260}$$

and

$$\left\langle y^2 \right\rangle = \alpha^2 \left\langle x^2 \right\rangle + 2\alpha\beta \langle xx' \rangle + \beta^2 \left\langle x'^2 \right\rangle \tag{261}$$

which give

$$\langle xy \rangle = 0 \tag{262}$$

and

$$\left\langle y^2 \right\rangle = \left\langle x^2 \right\rangle \tag{263}$$

in agreement with the conditions (52) and (53) for a symmetric distribution.

17 Appendix II

The following items are selected or entered on the TRIM user interface [5].

1. "Ion Distribution and Quick Calculation of Damage" option.
2. "Ion Distribution Only (no recoils) Projected on Y-Plane" option.
3. Hydrogen for the projectile ion.
4. 200 MeV for the ion kinetic energy.
5. 0 degrees for ion angle of incidence.
6. Carbon for the target material.
7. Target thickness in units of 10^{-6} or 10^{-10} meters.
8. 99999 for the number of ions. (This is the default value.)
9. "Transmitted Ions/Recoils" option.

The coordinate system used by TRIM is defined by three mutually orthogonal unit vectors $\widehat{\mathbf{x}}$, $\widehat{\mathbf{y}}$, and $\widehat{\mathbf{z}}$ with $\widehat{\mathbf{y}}$ and $\widehat{\mathbf{z}}$ in the plane of the target and $\widehat{\mathbf{x}}$ perpendicular to the target. For an incident angle of zero degrees, the direction of the incident ion is parallel to $\mathbf{x}$ (and therefore perpendicular to the target).

Let $\widehat{\mathbf{n}}$ be the unit vector parallel to the direction of an ion as it exits the target. In the $\widehat{\mathbf{x}}$, $\widehat{\mathbf{y}}$, $\widehat{\mathbf{z}}$ coordinate system one then has

$$\widehat{\mathbf{n}} = (\widehat{\mathbf{x}} \cdot \widehat{\mathbf{n}})\,\widehat{\mathbf{x}} + (\widehat{\mathbf{y}} \cdot \widehat{\mathbf{n}})\,\widehat{\mathbf{y}} + (\widehat{\mathbf{z}} \cdot \widehat{\mathbf{n}})\,\widehat{\mathbf{z}}. \tag{264}$$

The TRIM output file gives the values of

$$\mathrm{CX} = (\widehat{\mathbf{x}} \cdot \widehat{\mathbf{n}}), \quad \mathrm{CY} = (\widehat{\mathbf{y}} \cdot \widehat{\mathbf{n}}), \quad \mathrm{CZ} = (\widehat{\mathbf{z}} \cdot \widehat{\mathbf{n}}) \tag{265}$$

for each ion. Using these numbers one computes

$$\phi_y = \arctan(\mathrm{CY}/\mathrm{CX}), \quad \phi_z = \arctan(\mathrm{CZ}/\mathrm{CX}) \tag{266}$$

which are the desired angles ϕ_i. Note that since we are considering the emittance in just one plane, we can use the 99999 numbers for ϕ_x and ϕ_y as independent data sets. (I am indebted to P. Thieberger for pointing this out.)

References

[1] K.L. Zeno, "The Effect of the Booster Injection Foil on Emittance", C-A/AP/Note 177, October, 2004

[2] K.L. Zeno, "Booster and AGS Transverse Emittance during the 2006 and 2009 Polarized Proton Runs", C-A/AP/Note 404, September, 2010

[3] K.L. Zeno, "An Overview of Booster and AGS Polarized Proton Operation during Run 15", C-A/AP/Note 552, October, 2015

[4] K.A. Brown, et al, "Minimizing Emittance Growth during H-minus Injection in the AGS Booster", Proceedings of PAC09, Vancouver, BC, Canada, pp. 3729–3731.

[5] J.F. Ziegler, www.srim.org

[6] W.H. Press, "Numerical Recipes in Fortran", Second Edition, Cambridge University Press, 1994, p. 630

[7] C.J. Gardner, "Booster Stopband Corrections", Booster Technical Note No. 217, January 6, 1993

[8] I.S. Gradshteyn and I.M. Ryzhik, "Table of Integrals, Series, and Products", Corrected and Enlarged Edition, Academic Press, 1980, p. 337

[9] C.J. Gardner, "Projections of Beam Distributions", AGS/AD/Tech Note 439, July 11, 1996.

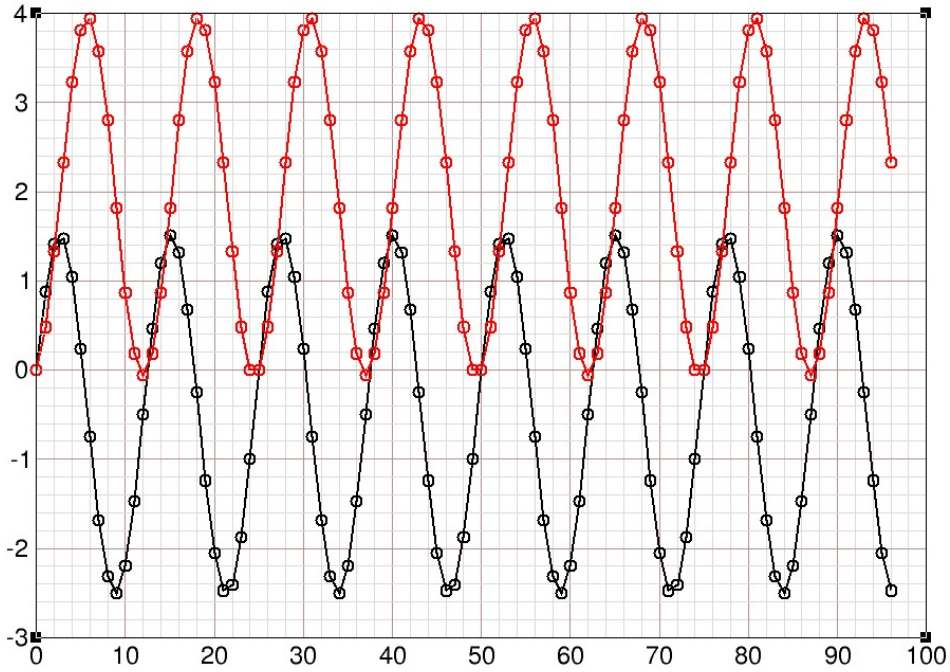

Figure 1: Coefficients $\mathcal{A}_n$ (black circles) and $\mathcal{B}_n$ (red circles) for tune $Q = 0.96$. The horizontal axis gives the turn number n. The curves connect the centers of the circles.

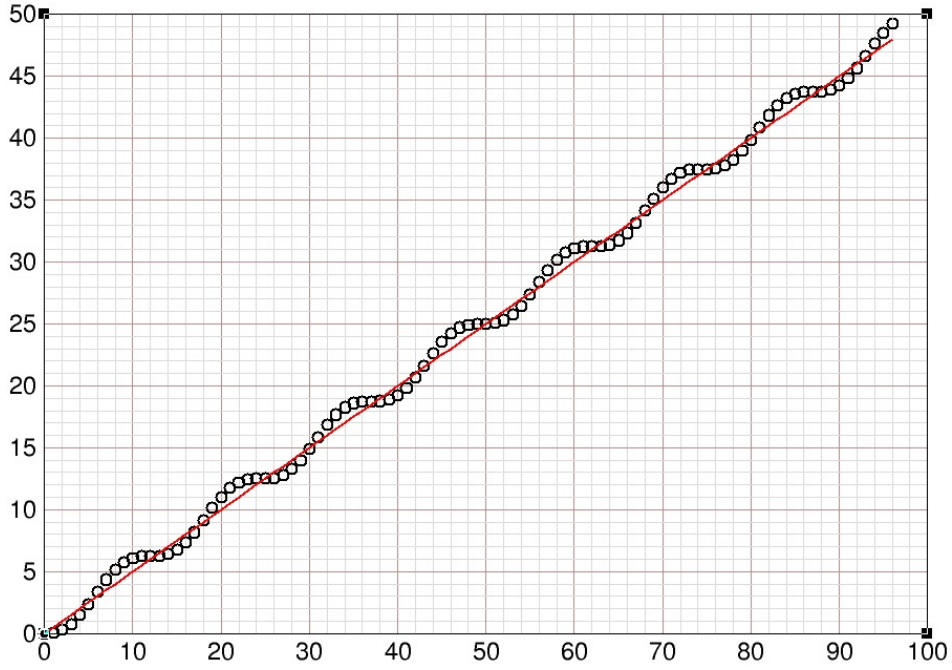

Figure 2: Function $F(n) = (n - \mathcal{A}_n)/2$ (black circles) for tune $\underline{Q = 0.96}$. The horizontal axis gives the turn number n. The red curve is the line $G(n) = n/2$. Here we see that the values of $F(n)$ simply oscillate about the line. As long as n is sufficiently large, the difference between $F(n)$ and $G(n)$ will be small compared to $F(n)$.

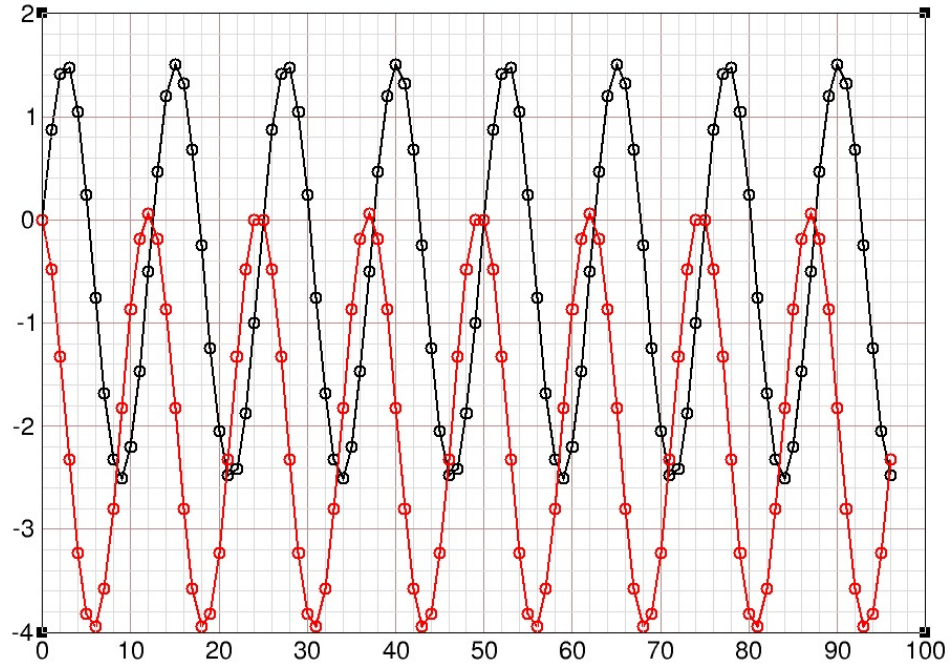

Figure 3: Coefficients $\mathcal{A}_n$ (black circles) and $\mathcal{B}_n$ (red circles) for tune $Q = 0.54$. The horizontal axis gives the turn number n. The curves connect the centers of the circles. Note that 0.54 and 0.96 are equidistant from but on opposite sides of 0.75. The coefficient $\mathcal{A}_n$ is the same for tunes with this symmetry. The coefficient $\mathcal{B}_n$ changes sign. This follows from equations (134), (137), and (138), and is easily verified by comparing the values plotted here with those plotted in **Figure 1**.

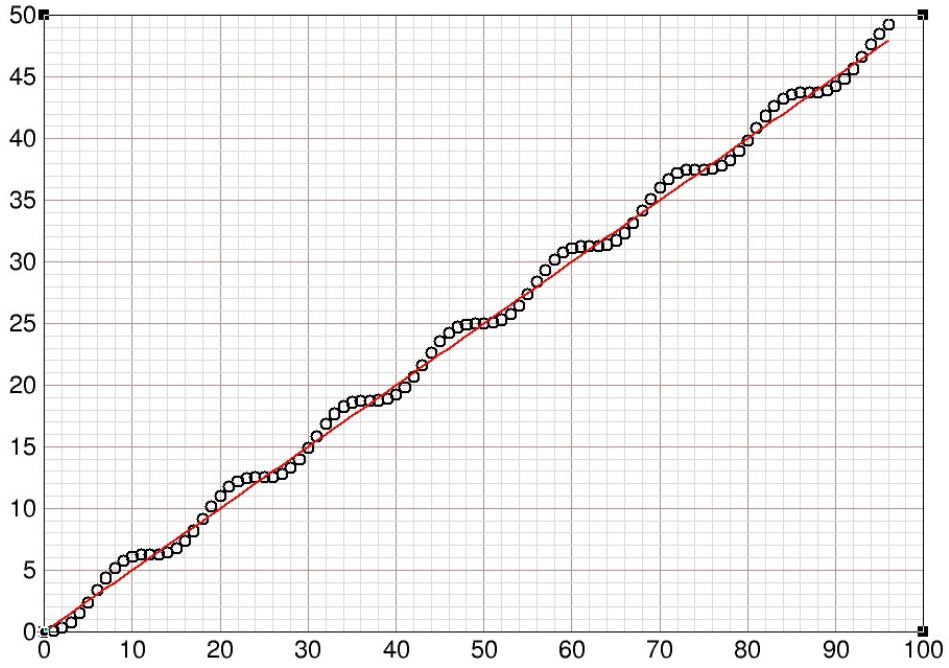

Figure 4: Function $F(n) = (n - \mathcal{A}_n)/2$ (black circles) for tune $\underline{Q = 0.54}$. The horizontal axis gives the turn number n. The red curve is the line $G(n) = n/2$. The values of $F(n)$ plotted here are the same as those plotted in **Figure 1**. This is because $\mathcal{A}_n$ is the same for $Q = 0.54$ and $Q = 0.96$.

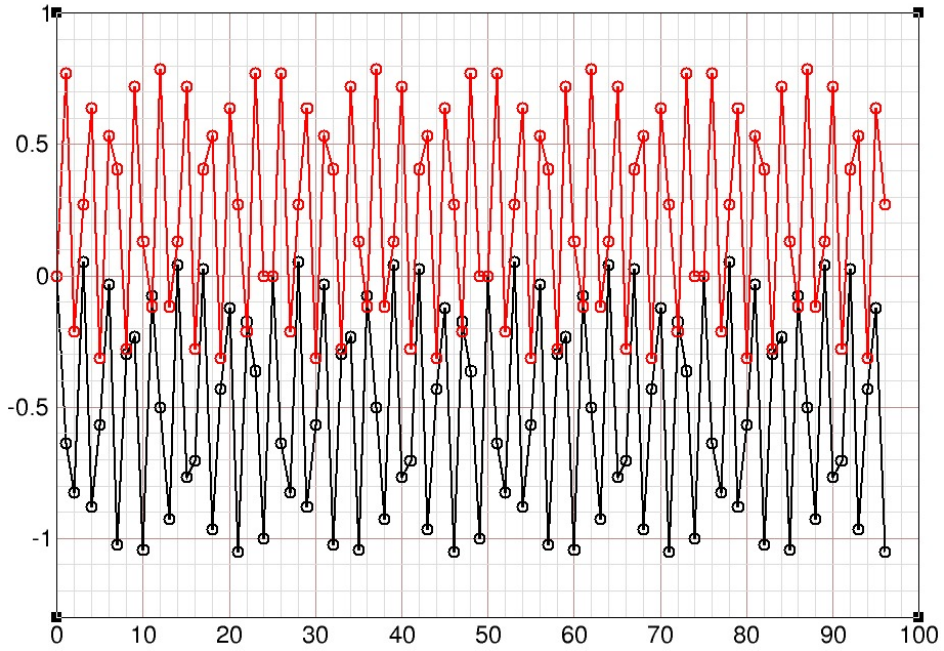

Figure 5: Coefficients $\mathcal{A}_n$ (black circles) and $\mathcal{B}_n$ (red circles) for tune $Q = 0.82$. The horizontal axis gives the turn number n. The curves connect the centers of the circles. The values plotted here are significantly smaller than those plotted in **Figures 1** and **3**. This is because the tune is well away from integer and half-integer values.

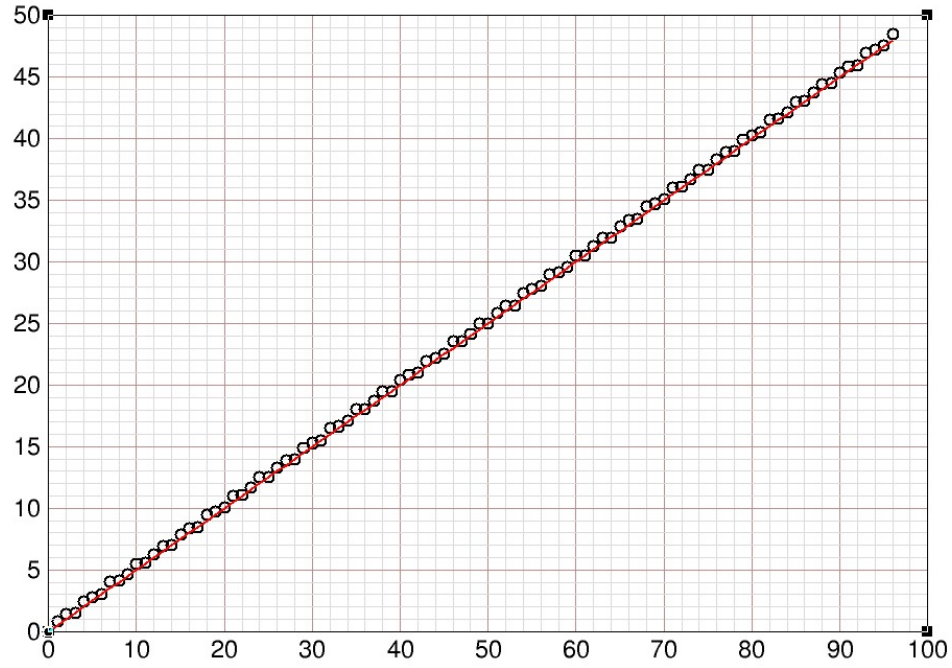

Figure 6: Function $F(n) = (n - \mathcal{A}_n)/2$ (black circles) for tune $Q = 0.82$. The horizontal axis gives the turn number n. The red curve is the line $G(n) = n/2$. The oscillations of $F(n)$ about the line are much smaller here because the tune is well away from integer and half-integer values.

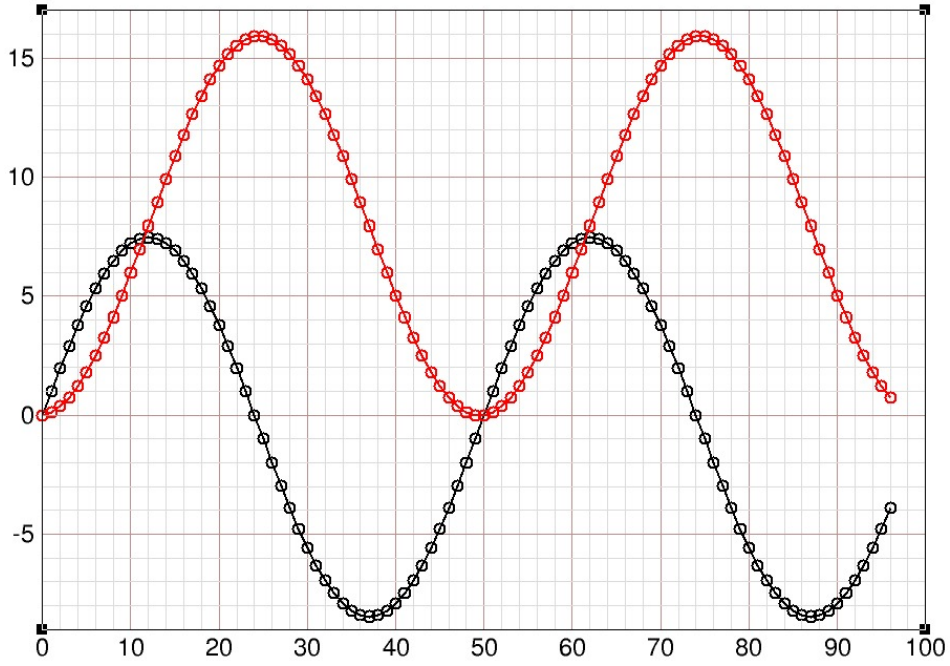

Figure 7: Coefficients $\mathcal{A}_n$ (black circles) and $\mathcal{B}_n$ (red circles) for tune $Q = 0.99$. The horizontal axis gives the turn number n. The curves connect the centers of the circles. The oscillation amplitudes are large here because the tune is very close to 1.

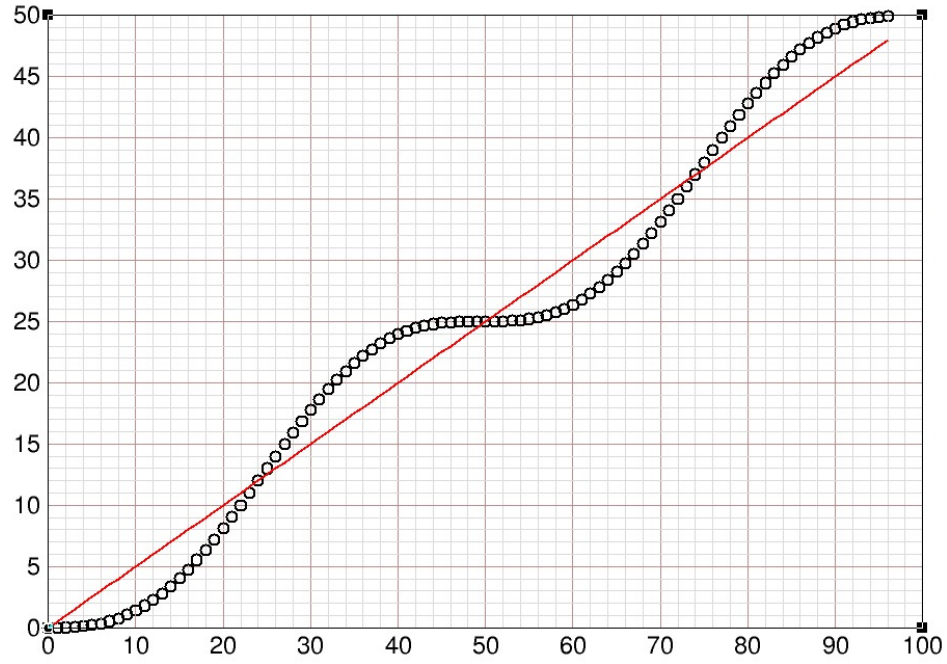

Figure 8: Function $F(n) = (n - \mathcal{A}_n)/2$ (black circles) for tune $Q = 0.99$. The horizontal axis gives the turn number n. The red curve is the line $G(n) = n/2$. The oscillations of $F(n)$ about the line are large because the tune is very close to 1.

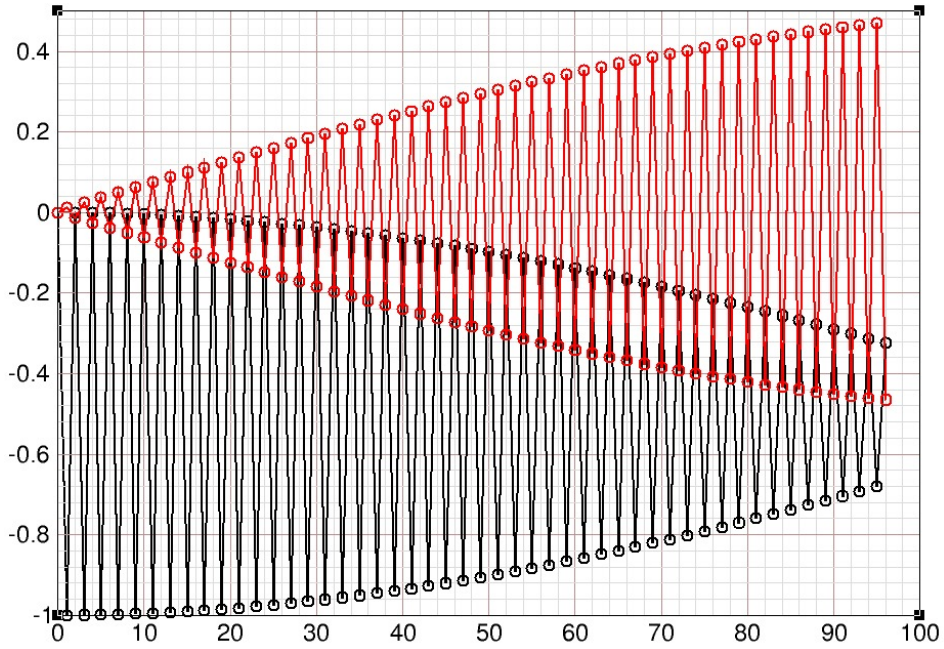

Figure 9: Coefficients $\mathcal{A}_n$ (black circles) and $\mathcal{B}_n$ (red circles) for tune $Q = 0.751$. The horizontal axis gives the turn number n. The curves connect the centers of the circles. Here the tune is well away from 0.5 and 1.

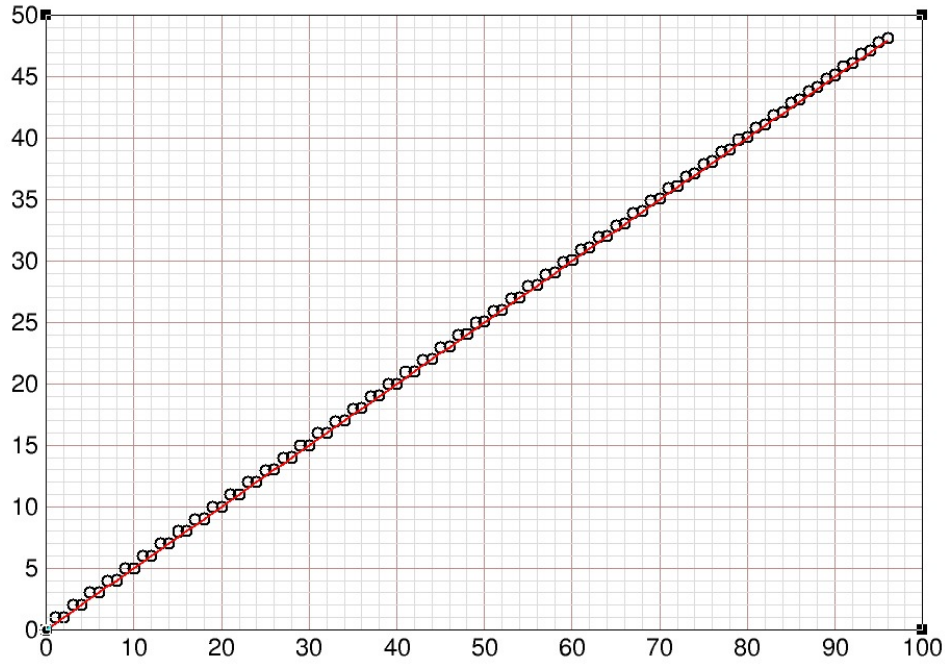

Figure 10: Function $F(n) = (n - \mathcal{A}_n)/2$ (black circles) for tune $\underline{Q = 0.751}$. The horizontal axis gives the turn number n. The red curve is the line $G(n) = n/2$. The oscillations of $F(n)$ about the line are small here because the tune is well away from 0.5 and 1.

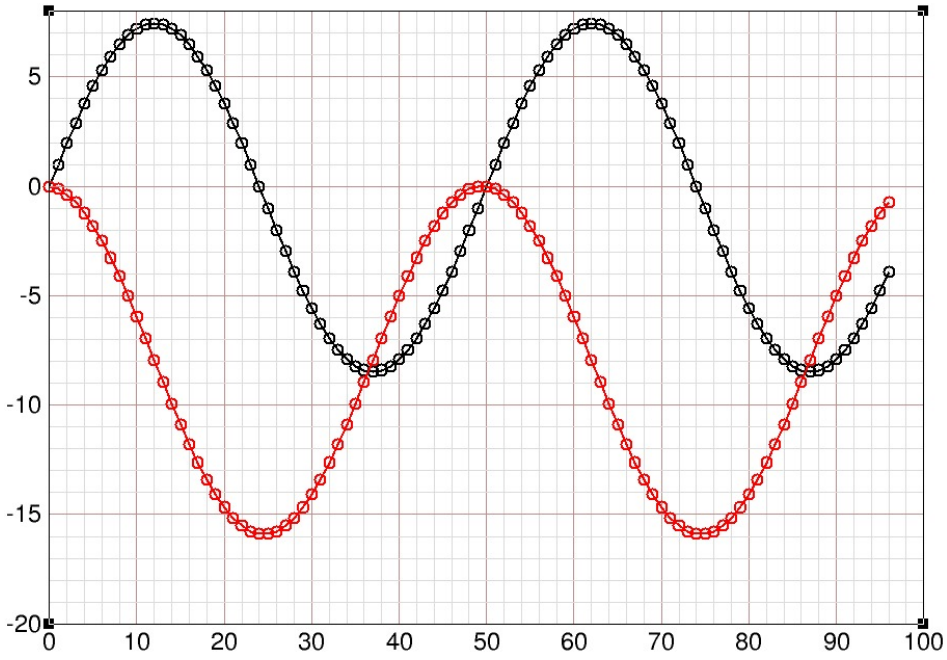

Figure 11: Coefficients $\mathcal{A}_n$ (black circles) and $\mathcal{B}_n$ (red circles) for tune $Q = 0.51$. The horizontal axis gives the turn number n. The curves connect the centers of the circles. The oscillation amplitudes are large here because the tune is very close to 0.5.

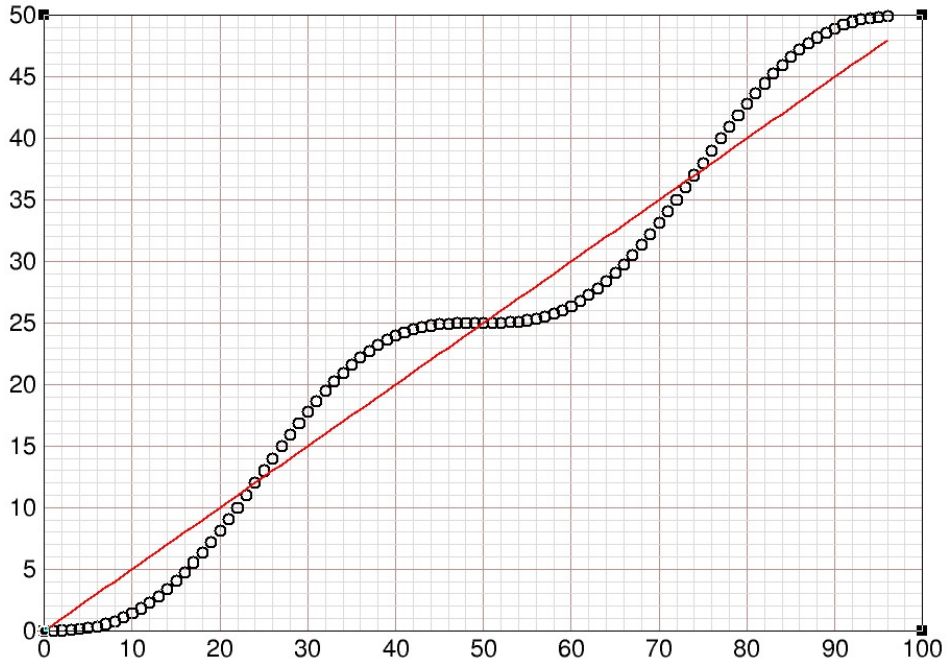

Figure 12: Function $F(n) = (n - \mathcal{A}_n)/2$ (black circles) for tune $Q = 0.51$. The horizontal axis gives the turn number n. The red curve is the line $G(n) = n/2$. The oscillations of $F(n)$ about the line are large because the tune is very close to 0.5.

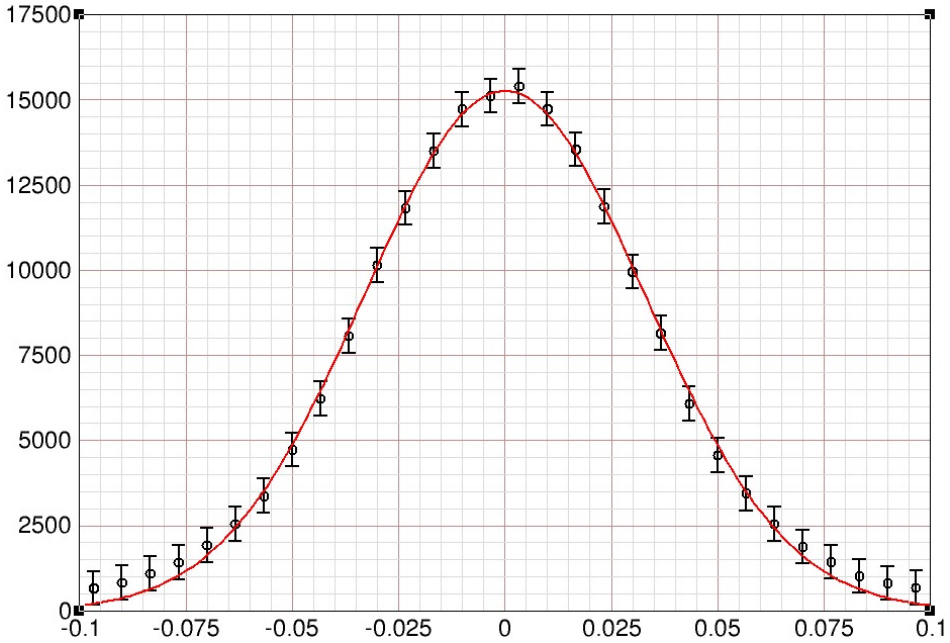

Figure 13: Distribution of scattering angles for 200 MeV protons incident on a 200 microgram per cm^2 carbon foil. The horizontal axis gives the scattered proton angle in milliradians (mr). The vertical axis gives the number of scattered protons for a given angle. The black circles represent data from TRIM that has been binned. The red curve is the fitted Gaussian. The indicated error bars were chosen to be ± 500 for convenience. The rms angles obtained from (199) and from the fitted Gaussian are 0.0344 and 0.0331 mr, respectively. In order to get agreement between these two numbers, the angular data from TRIM had to be restricted to the range indicated by the red curve.

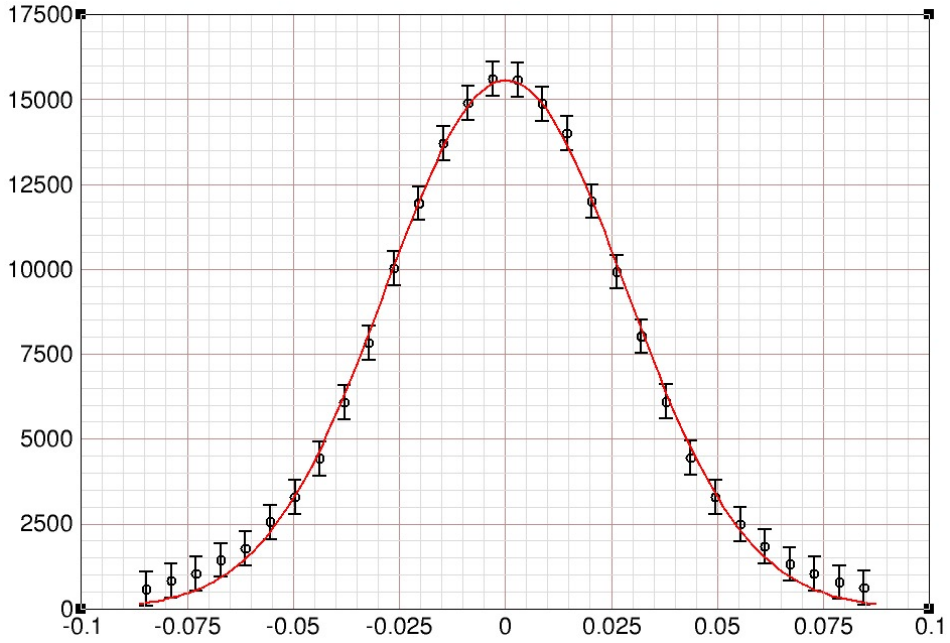

Figure 14: Distribution of scattering angles for 200 MeV protons incident on a 150 microgram per cm^2 carbon foil. The horizontal axis gives the scattered proton angle in milliradians (mr). The vertical axis gives the number of scattered protons for a given angle. The black circles represent data from TRIM that has been binned. The red curve is the fitted Gaussian. The indicated error bars were chosen to be ± 500 for convenience. The rms angles obtained from (199) and from the fitted Gaussian are 0.0297 and 0.0283 mr, respectively. In order to get agreement between these two numbers, the angular data from TRIM had to be restricted to the range indicated by the red curve.

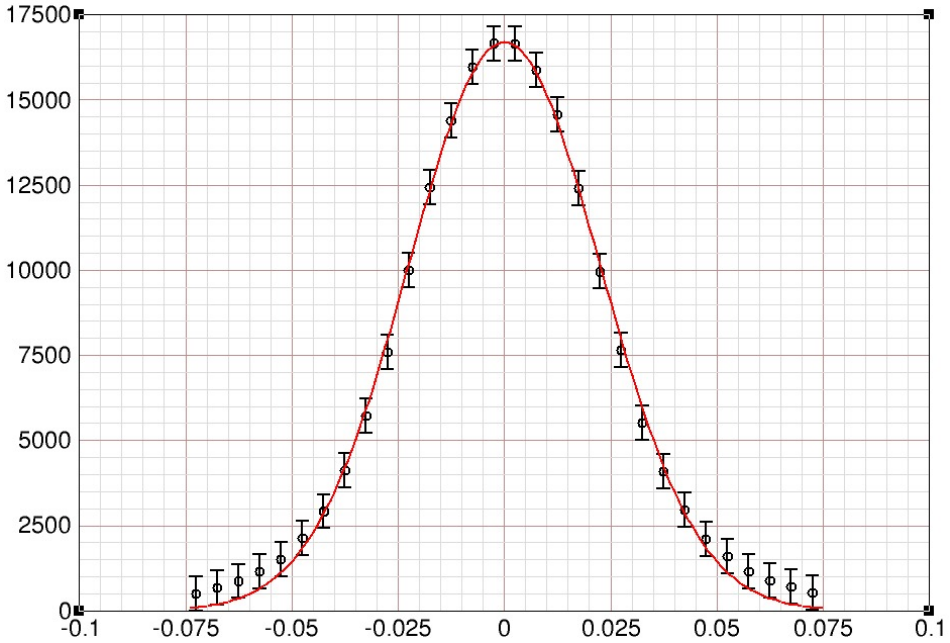

Figure 15: Distribution of scattering angles for 200 MeV protons incident on a 100 microgram per cm^2 carbon foil. The horizontal axis gives the scattered proton angle in milliradians (mr). The vertical axis gives the number of scattered protons for a given angle. The black circles represent data from TRIM that has been binned. The red curve is the fitted Gaussian. The indicated error bars were chosen to be ± 500 for convenience. The rms angles obtained from (199) and from the fitted Gaussian are 0.0243 and 0.0226 mr, respectively. In order to get agreement between these two numbers, the angular data from TRIM had to be restricted to the range indicated by the red curve.

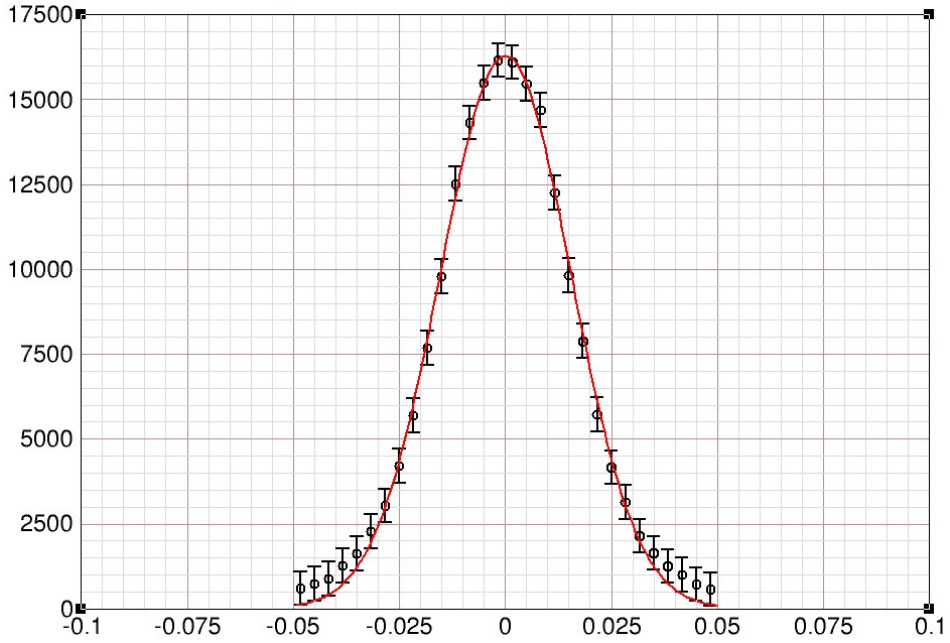

Figure 16: Distribution of scattering angles for 200 MeV protons incident on a 50 microgram per cm^2 carbon foil. The horizontal axis gives the scattered proton angle in milliradians (mr). The vertical axis gives the number of scattered protons for a given angle. The black circles represent data from TRIM that has been binned. The red curve is the fitted Gaussian. The indicated error bars were chosen to be ± 500 for convenience. The rms angles obtained from (199) and from the fitted Gaussian are 0.0165 and 0.0154 mr, respectively. In order to get agreement between these two numbers, the angular data from TRIM had to be restricted to the range indicated by the red curve.

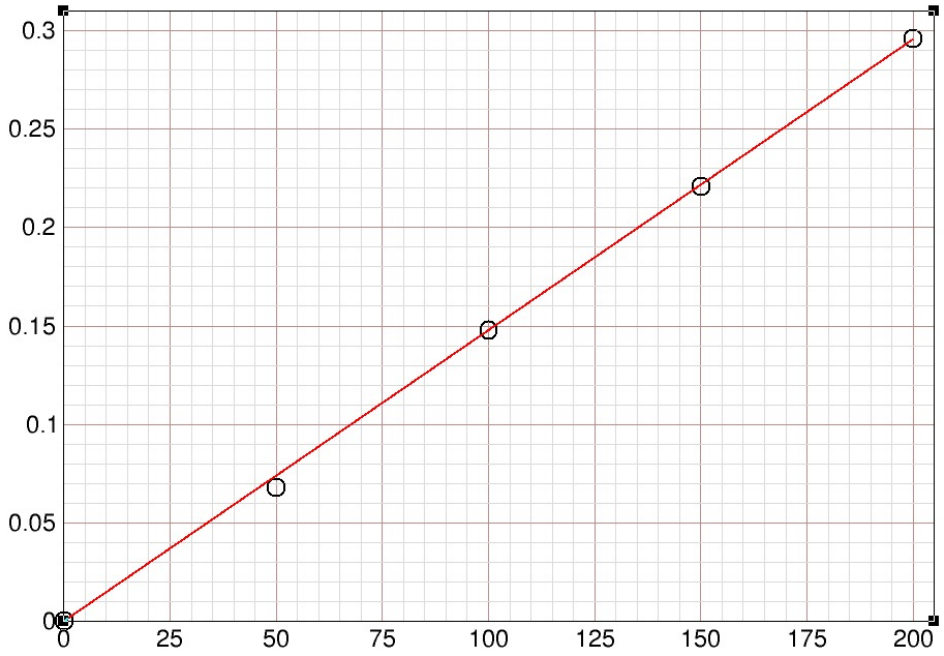

Figure 17: Emittance growth versus thickness of carbon foil. The black circles show the emittance growth given by (207) for foils of 200, 150, 100, and 50 microgram per cm^2 thickness. The vertical axis gives the emittance growth in mm mrad. The horizontal axis gives the foil thickness in micrograms per cm^2. The red curve is the straight line that connects the circle at 0 with the circle at 200 micrograms per cm^2. The slope of the line is $\mathcal{M} = 0.296/200$, which gives emittance growth $\mathcal{E}_n - \mathcal{E}_0 = \mathcal{M}\mathcal{T}$ for foil thickness $\mathcal{T}$.

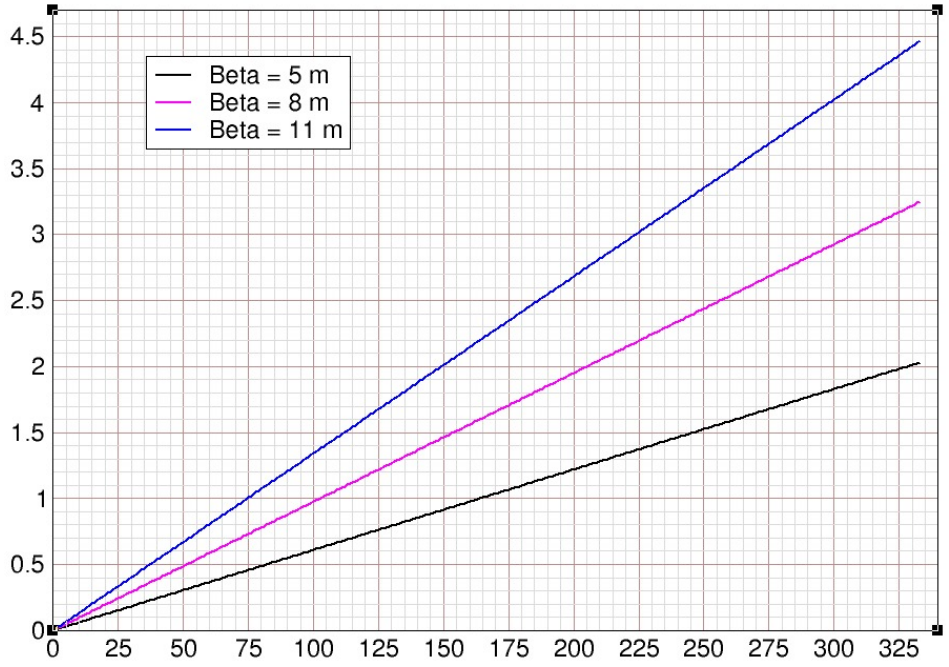

Figure 18: Emittance growth (212) versus turn for 100 microgram per cm^2 carbon foil. The black, magenta, and blue lines give, respectively, the growth for 5, 8, and 11 m lattice beta at the foil. The vertical axis gives the normalized emittance growth $(6\mathcal{E}_n - 6\mathcal{E}_0)_N$ in mm mrad. The horizontal axis gives the turn number. The revolution period of 200 MeV protons in Booster is 1.1888 microseconds, which gives a time interval of 396 microseconds for the 333 plotted turns.

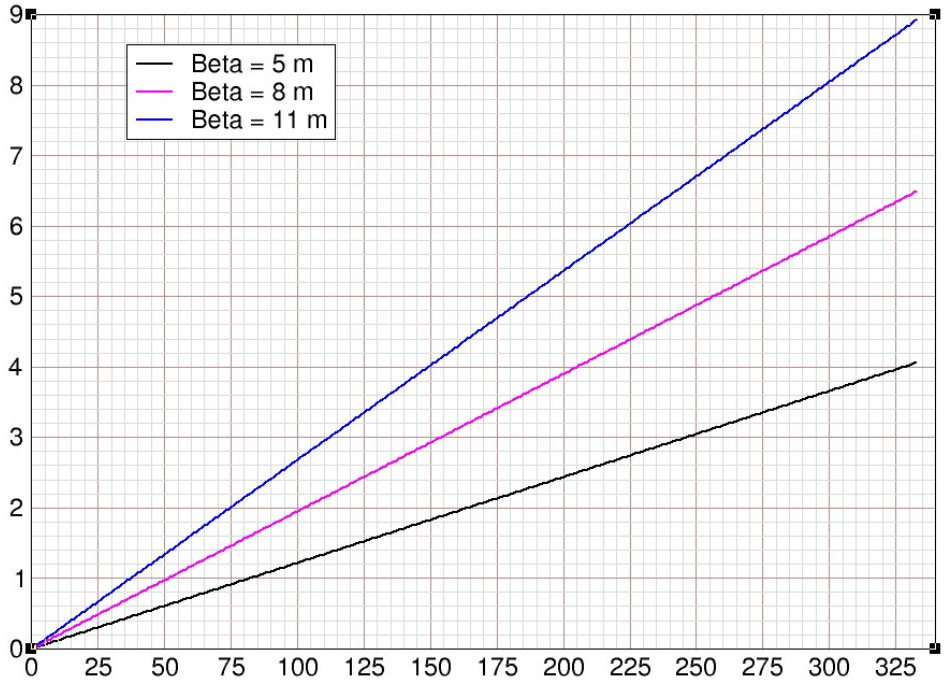

Figure 19: Emittance growth (212) versus turn for 200 microgram per cm^2 carbon foil. The black, magenta, and blue lines give, respectively, the growth for 5, 8, and 11 m lattice beta at the foil. The vertical axis gives the normalized emittance growth $(6\mathcal{E}_n - 6\mathcal{E}_0)_N$ in mm mrad. The horizontal axis gives the turn number. The revolution period of 200 MeV protons in Booster is 1.1888 microseconds, which gives a time interval of 396 microseconds for the 333 plotted turns.